# 3 Nanocrystallization and Nanoprecipitation Technologies

Vivek P. Patel, Dhara V. Patel, and Jayvadan K. Patel

**Abstract**

In the last few years, nanoparticles and their applications have dramatically diverted science in the direction of a brand new philosophy. Nanoparticles are building the bridge of scientific knowledge connecting bulk materials to atomic or molecular structures. In the present scenario, nanoparticle research is a very promising branch of scientific research owing to the wide range of potential and promising applications especially in biomedical, optical and electronic fields.

In the current pharmaceutical development pipeline, the poor water solubility of drug candidates remains the biggest challenge. Various processes have been developed to increase the solubility, dissolution velocity and bioavailability of these active ingredients belonging to the biopharmaceutical classification system (BCS) II and IV classifications. Nanocrystal delivery is an emerging technique for overcoming the limitations of drugs that dissolve poorly in water. Nanocrystals are produced in the form of nanosuspensions using top-down (e.g., wet milling) and bottom-up methods (e.g., antisolvent precipitation) in FDA-approved drug products. An ultra cryo-milling technique using liquid nitrogen and dry ice beads has been used as a novel contamination-free process. In the case of the antisolvent precipitation technique, ultrasound and rapid mixing devices have been used as new process intensification techniques. Technological advancements in milling as well as ant solvent precipitation now enable the production of drug nanoparticles on a commercial scale with relative ease.

This chapter provides an updated review of nanocrystal techniques along with marketed product evaluations and a survey of the commercially relevant scientific literature.

**Keywords**

Nanoparticles · Nanocrystallization · Nanomilling · Antisolvent precipitation

V. P. Patel (✉)
Sun Pharmaceutical Industries Ltd,
Vadodara, Gujarat, India
e-mail: vivek.patel@sunpharma.com

D. V. Patel
Pioneer Pharmacy Degree College,
Vadodara, Gujarat, India

J. K. Patel
Nootan Pharmacy College,
Sankalchand Patel University,
Visnagar, Gujarat, India



J. K. Patel, Y. V. Pathak (eds.), *Emerging Technologies for Nanoparticle Manufacturing*,
https://doi.org/10.1007/978-3-030-50703-9_3

## 1 Introduction

Nanotechnology is a recent hot topic because of its potential to have an appreciable impact on a number of fields related to biology, chemistry, engineering, as well as medicine.

In the current scenario, approximately 90% of new drug candidates in the development pipeline can have a poor solubility problem that leads to poor dissolution velocity and ultimately variable bioavailability. These new drug candidates belong to biopharmaceutical classification systems (BCS) class II (70%) and class IV (20%). Over the last 10 years, progress in high-throughput screening methods has led to an even higher number of newly discovered drug candidates that have poor water solubility problems (Gigliobianco et al. 2018; Junghanns and Müller 2008; Loftsson and Brewster 2010; Müller and Keck 2012). Given the higher number of poorly bioavailable drug candidates and their non-specific distribution throughout the body may lead to different side effects and may further limit their clinical applications. To overcome the bioavailability issue of drug candidates, appropriate innovative formulation technologies according to the route of administration, e.g., oral and non-oral, need to be adopted (Trapani et al. 2012; Lu et al. 2016a; Keck and Müller 2006).

In the previous era, micronization was used to reduce the particle size and led to an increase in the dissolution velocity of poorly soluble drug candidates. But still, micronization cannot fulfill the needs and satisfy the pharmaceutical requirements to improve the dissolution velocity as well as the bioavailability of drug candidates. The demand for these pharmaceuticals makes the changeover to nanonization. Different and unique innovative nanonization approaches that have emerged to reduce the particle size and improve the dissolution velocity tend to increase the bioavailability of poorly soluble drug candidates for target therapy. These unique innovative technological approaches help to overcome the physicochemical characteristics, including stability issues, that are associated with nanostructures (Jermain et al. 2018).

In this chapter, emerging manufacturing techniques for drug nanoparticles are briefly introduced, followed by a detailed review of the progress of targeted drug delivery. A short introduction with recent advancements in conventional technologies for nanoparticle manufacturing is also included.

## 2 Definition

The classical definition of "nanocrystals" is crystals with a nanometer size range, typically between a few nanometers and a thousand nanometers and is crystalline in nature. Another characteristic is that they are made up of 100% drug crystals or with a minimal amount of surface stabilizing agents such as surfactant or polymeric carrier stabilizers. Drug nanocrystals, when suspended in dispersion media, are called "nanosuspension." Dispersion media can be either aqueous (e.g., water-based dispersion system) or non-aqueous (e.g., different vegetable oils, polyethylene glycol, polypropylene glycol, and solvents). As per the biopharmaceutical classification systems (BCS), class II drugs are the most prominent candidates for drug nanocrystals, but in some cases class IV drugs may have even more benefits when particle size is decreased.

Nowadays, nanosuspension formulations are used to increase the dissolution velocity and saturation solubility of drug candidates belonging to BCS classes II and IV. Because of the nano-range particles with increased specific surface area, nanosuspensions have unique biological effects. Based on the above-mentioned physicochemical and biological beneficial effects, the US FDA has approved several nanosuspension medications and these are currently marketed well. Owing to the factual information given above, we can say that nanosuspensions are a mature drug delivery system.

"Nanoparticles" are drug-embedded particles in a nanometer size range, but mainly include polymers or lipids, such as polymeric nanoparticles, liposomes, and solid lipid nanoparticles. Nanoparticles can be in either a crystalline or an amorphous physical state, which depends on the

nanoparticle formation technologies. In precipitation techniques, the nanoparticles are generally obtained in an amorphous physical state. Thus, eventually, amorphous drug nanoparticles should not be referred to as nanocrystals (Liu et al. 2012; Peltonen and Hirvonen 2018; Borchard 2015; Gao et al. 2012; Kesisoglou et al. 2007; Liu et al. 2011). Amorphous drug nanoparticles have certain advantages, e.g., it has higher saturation solubility than equally sized nanocrystals. Furthermore, a unique combination of nanometer size range as well as amorphous state is considered ideal for drug candidates to reach the highest saturation solubility. However, to utilize the concept in the pharmaceutical field, it should be equally as important to maintain the amorphous state throughout the shelf-life of product (Hancock and Parks 2000; Gu and Grant 2001).

## 3 Prominent Attributes

### 3.1 Surface Area Enlargement

The main idea of nanotechnology is the ratio of surface area to volume. Surface area is increased, whereas the volume remains the same. Moreover, it can be explained as follows: an increase in the particle surface area leads to an increased possibility of having a reaction (with atmosphere or gases or liquid/dissolution solvents around the nanoparticles, etc.). Size reduction via micronization to nanonization (Fig. 3.1) leads to a drastic increase in the surface area and thus the possibility of having a reaction with liquid/dissolution solvents is also increased drastically, or what we call increased dissolution velocity, according to the Noyes–Whitney equation (Eq. 3.1) (Noyes and Whitney 1897).

$$\frac{dC}{dt} = \frac{DS}{Vh}\left(Cs - Cx\right) \tag{3.1}$$

*dC/dt*, dissolution rate (concentration change as a function of time); *D*, diffusion coefficient; *S*, surface area; *V*, dissolution volume; *h*, diffusion layer thickness; *Cs*, saturation concentration; *C*, concentration at time *t*.

Thus, if considering a particle size reduction from 1 mm (typical particle size for conventional drugs) to 100 nm (typical particle size for drug nanocrystals), then the dissolution velocity is increased 100-fold.

This reflects the fact that the particle size has become an important factor for the determination of dissolution velocity. However, when the dissolution parameter tests are performed under specific dissolution sink conditions, the differences are difficult to identify in numbers between different nanocrystal size fractions; thus, it required a more discriminating dissolution test protocol (Liu et al. 2013).

Therefore, surface area enlargement is the correct way to improve the bioavailability of BCS class II and IV drug candidates where the solubility and dissolution velocity is the rate limiting step. It also seems in most the cases that low dissolution velocity correlates directly with low saturation solubility (Owais et al. 2019; Alshora et al. 2016).

### 3.2 Increase in Saturation Solubility

Ideally, saturation solubility of drug candidates is dependent on the specific dissolution sink conditions, which include dissolution medium, the concentration of the buffers, pH, and temperature. This is valid up to the micrometer range or above the size of the drug candidates. However, saturation solubility also depends on particle sizes of below approximately 1 μm. Saturation solubility increases with decreasing particle size below 1 μm. Also, according to the Noyes–Whitney equation the dissolution rate dC/dt is proportional to the concentration gradient (Cs − Cx)/h (Cs – saturation solubility, Cx – bulk concentration, h – diffusional distance) and therefore the dissolution velocity is further increased. At the same time, increased saturation solubility also increases the concentration gradient between the gut lumen and the blood, which leads to higher absorption by the passive diffusion mechanism (Fig. 3.2).

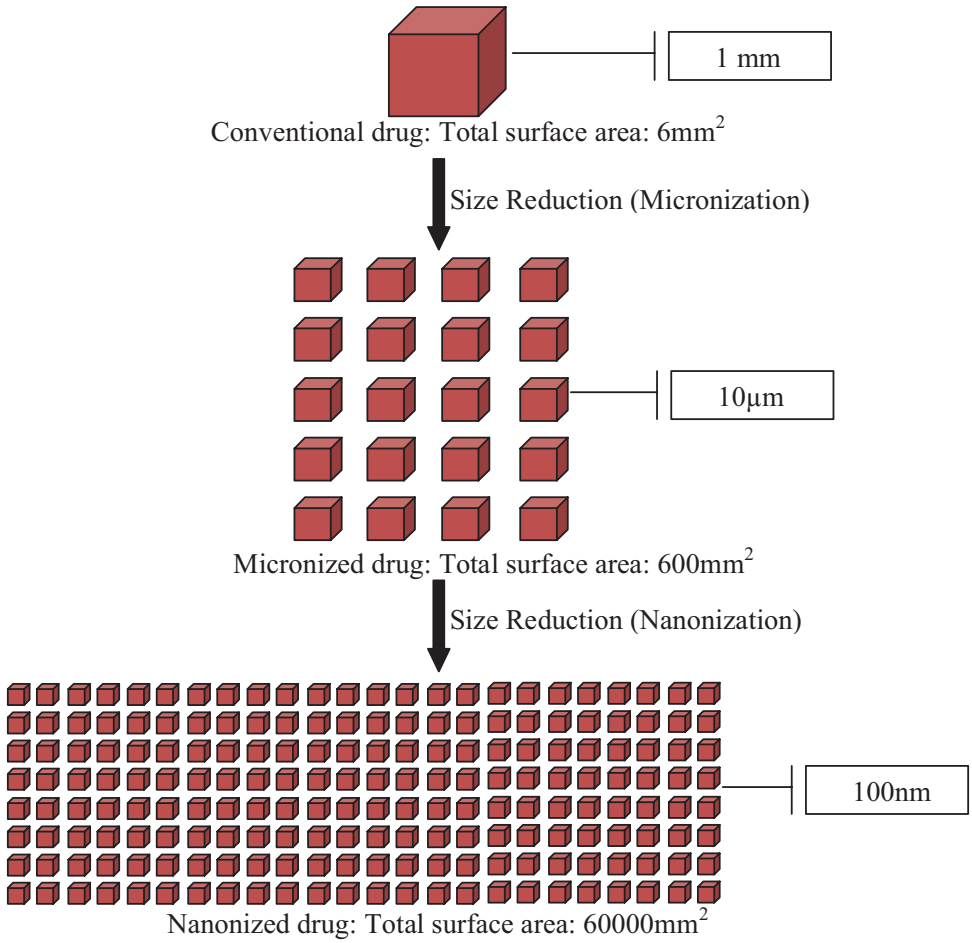


**Fig. 3.1** Surface enlargement factor and increase in the number of crystals by size reduction

Generally, the diffusion layer starts to get thinner for particle sizes below approximately 50 µm (Sheng et al. 2007), which furthermore become thinner for particle sizes in the nanometer range and hence enhances the dissolution velocity of nanoparticles compared with microparticles.

According to the Ostwald–Freundlich theory, for particle sizes below approximately 1 µm, the saturation concentration starts to increase. The increasing effect on saturation concentration is more pronounced once the particle size is below 100 nm. Drug saturation solubility is theoretically predicted by the Ostwald–Freundlich equation (Eq. 3.2):

$$S_{\mathrm{NP}} = S_0 \exp\left(\frac{2V_m\gamma}{RTr}\right) \tag{3.2}$$

Where $S_{NP}$ is the solubility of nanoparticles with a radius $r$, $S_0$ is the solubility of bulk material, $V_m$ is the molar volume, $\gamma$ is the interfacial tension, $R$ is the gas constant and $T$ is the temperature.

In his dissertation of 1885, Robert von Helmholtz (son of the German physicist Hermann

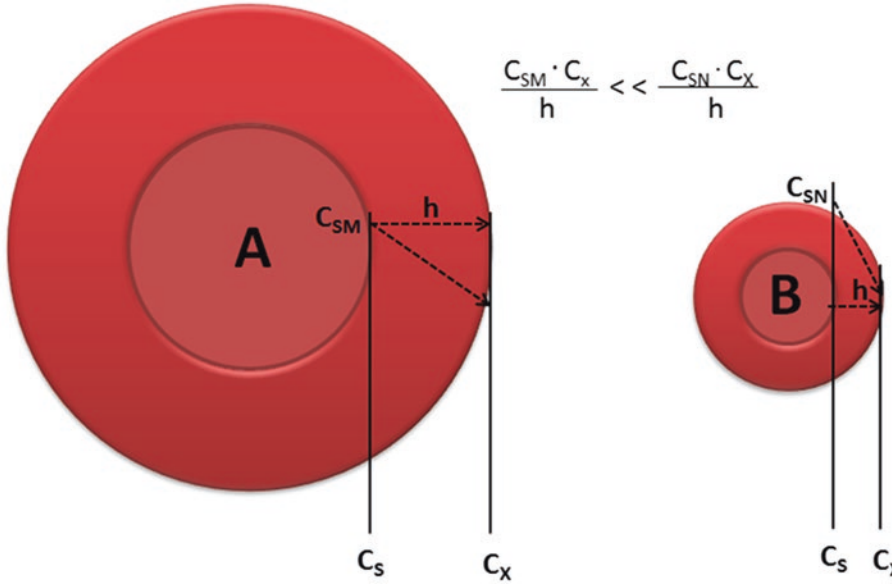


**Fig. 3.2** Comparison of (**a**) a microcrystal and (**b**) a nanocrystal and their surface curvature and concentration gradient over the diffusional distance (h). $C_s$, drug-saturated water at surface (M, microcrystal; N, nanocrystal); $C_x$, bulk concentration at diffusional distance; h, diffusional distance. $dc/dt \sim (C_s - C_x)/h$

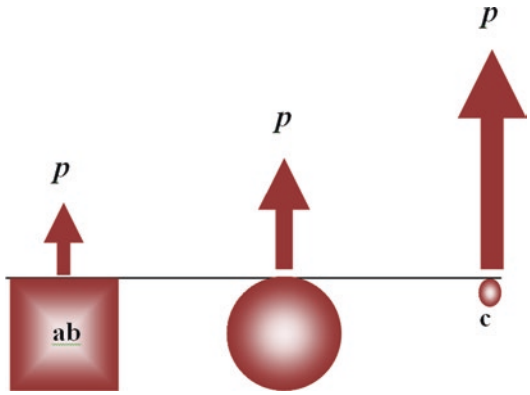


**Fig. 3.3** Dissolution pressure (*p*) increased over (**a**) a flat surface, (**b**) a microparticle, and (**c**) a nanoparticle with a high surface curvature

von Helmholtz) achieved the Ostwald–Freundlich equation and explained that Kelvin's equation could be translated into the Ostwald–Freundlich equation (Helmholtz 1886). One aftermath is that small liquid droplets (i.e., particles with more surface curvature or nanoparticles) exhibit a more effective vapor pressure, because the surface is bigger in comparison with the volume. Now, consider that the vapor pressure is equivalent to the dissolution pressure for nanoparticles in liquid; there should be an equilibrium of molecules dissolving and molecules recrystallizing in the state of saturation solubility. This equilibrium can be moved if the dissolution pressure increases, and hence the saturation solubility increases (Fig. 3.3).

The advantageous effect of nanoparticles, the increased dissolution velocity, and the increased saturation concentration all lead to a supersaturated state and ultimately this increases the drug absorption as well as permeation (Brouwers et al. 2007, 2009; Mellaerts et al. 2008).

The biggest challenge faced by scientists during development is to maintain the supersaturated state in vivo until absorption and permeation have taken place, because there is the highest probability of interference via uncontrolled precipitation or crystallization (Peltonen and Hirvonen 2018).

### 3.3 Crystalline or Amorphous Particle States

Based on the drug delivery applications of drug candidates, crystalline or amorphous particle states are anticipated to prevent or enhance the solubility, dissolution velocity, and pharmacokinetic profile.

The combination of nanometer size and amorphous state of drug candidate is ideal for higher saturation solubility compared with equally sized nanocrystals, but at the same time it is required to be maintained throughout the shelf-life of the product.

Concurrently, the importance of crystalline nanoparticles to the pharmaceutical field can be evaluated by the fact that more than 20 formulations are already on the market and approximately 15–20 are at different stages of clinical trials (Kumar and Burgess 2012).

To calculate the optimal nanosize and crystalline/amorphous state of the drug candidate, keep in mind the following parameters:

- Different administration route (oral, intravenous, intramuscular, pulmonary, ocular, dermal, etc.) (Chen et al. 2014; Fu et al. 2013; Ige et al. 2013; Mauludin et al. 2009; Colombo et al. 2017; Zhai et al. 2014; Vidlářová et al. 2016; Mitri et al. 2011; Muller and Keck 2004; Ganta et al. 2009; Patravale et al. 2004; Shegokar and Singh 2011; Gao et al. 2016; Khan et al. 2013; Liu et al. 2010a, 2018; Yang et al. 2010; Zhao et al. 2011).
- Different pharmaceutical dosage forms (tablets, capsules, suspensions, ointments, etc.) (Baba et al. 2007; Liversidge and Cundy 1995; Merisko-Liversidge et al. 1996; Moschwitzer and Muller 2006; Yang et al. 2017).
- Preservation of physical and chemical stability (Hancock and Parks 2000; Merisko-Liversidge and Liversidge 2011; Trasi and Byrn 2012; Lee 2003; Van Eerdenbrugh et al. 2008).
  - Different lattice arrangements such as short-, long-range order (Kreuter et al. 1995).
  - Glass transition temperature (Tg), X-ray diffraction, birefringence characteristic, melting event, etc.
  - Presence of stabilizers such as polymers, surfactants, and sugars.
- Commanded pharmacokinetics profile.
  - Long circulating and favorable biological properties (Wang et al. 2018; Sharma et al. 2016; Lu et al. 2016b).
  - Potential for passive and active targeting (Huang et al. 2010; Pawar et al. 2014).

## 4 Production Technologies

Previously, physical and chemical methods were only used to produce nanoparticles. Some of the commonly used physical and chemical methods are solvothermal synthesis, reduction, ion sputtering, and sol gel technique. Basically, there are two main approaches to nanoparticle synthesis; namely, bottom-up approaches and top-down approaches.

Top-down approaches involve the reduction of large particles to the nanometer size range, for example, by milling, whereas bottom-up methods generate nanoparticles by fabricating them from drug molecules in solution, such as by precipitation (Fig. 3.4). Some approaches defined as combined technologies involve the application of two technologies in succession.

Top-down techniques, particularly media milling and high-pressure homogenization, have

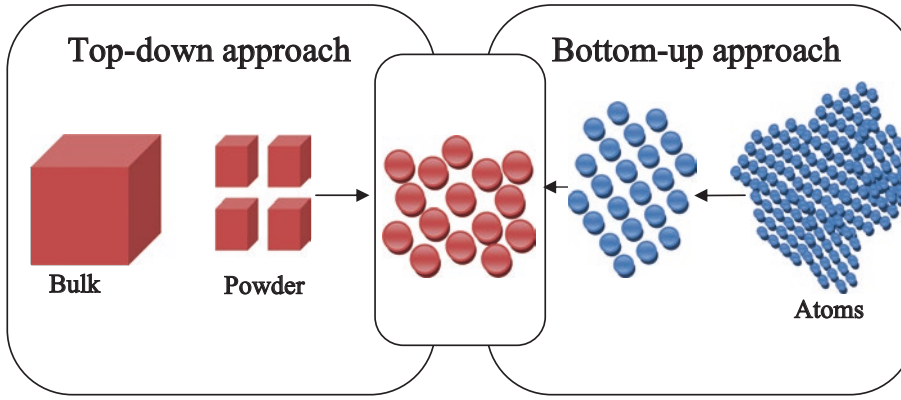


**Fig. 3.4** Top-down and bottom-up approaches of nanofabrication

become increasingly recognized by the pharmaceutical industry because it was easy to scale up to a commercial level. Top-down processes are universal techniques for preparing crystalline nanoparticles and have also been accepted by the regulatory authorities (Rabinow 2004).

Bottom-up technologies (i.e., starting from a dissolved molecule, precipitation) were difficult to control the process during scale up. One of the reasons was to remove the solvents and to control the process. The reality was that many poorly soluble drugs were poorly soluble not only in aqueous media but also in organic solvent media (Rawat 2015; Muller et al. 2001).

## 5 Nanocrystallization and Nanoprecipitation Technologies

Research and development (R&D) and the pharmaceutical industry have to focus their efforts on optimizing scalable processes and formulations, and allow for an appropriate physicochemical and biological stability during the shelf life of the drug product.

## 6 Media Milling

A milling/grinding chamber, milling media, milling shaft, motor, screen, recirculating chamber, and coolant are the major components of the wet media milling process (Fig. 3.5). The milling chamber can be constructed in a horizontal or a vertical position. In the process, the milling chamber is filled to 70–90% with milling beads sized 0.03–30 mm. The milling beads are made of different materials as needed, such as yttrium-stabilized zirconium oxide, stainless steel, glass alumina, titanium, or certain polymers, such as highly cross-linked polystyrene and methacrylate. Milling/grinding beads are generally available in spherical and cylindrical forms. The milling chamber is filled with slurry containing the drug, water, stabilizers, and surfactants agitated by the motor. The slurry occupies approximately 3–30% (w/v) volume of the milling chamber. The activation of the milling beads occurs by use of an agitator shaft with pegs, disks or smooth-shaped agitating elements. The milling media roll over inside the milling chamber during agitation, generating high energy forces by shearing and impacting large drug crystals to

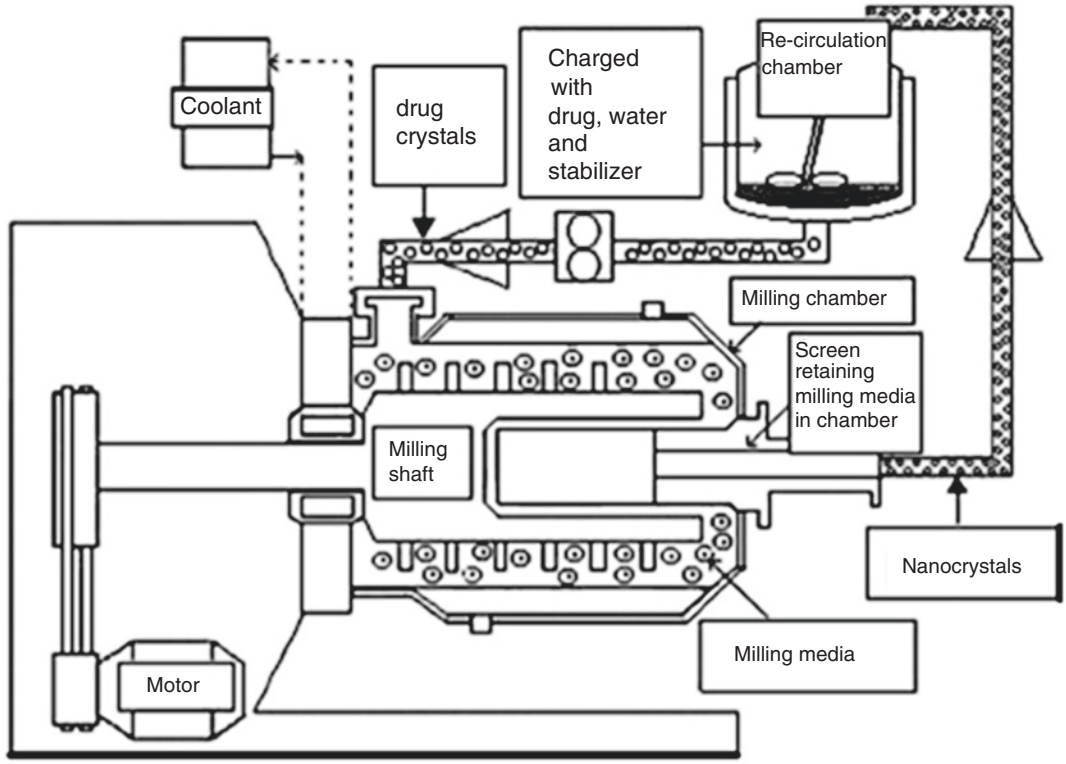


**Fig. 3.5** Schematic diagram describing the continuous wet bead milling process with a single chamber

reduce the particle size. Separation of the milling media from the product is done with the help of a screen at the outlet by separation (Yadav et al. 2012; Malamatari et al. 2018; Stenger and Peukert 2003; Kwade 1999). The milling operation can be performed, depending on the production scale and other formulation requirements, either in batch mode (discontinuous mode-single pass processing through one or more mills) (Fig. 3.6) or in recirculation mode (continuous mode-circulation processing with a single vessel). Recirculation is advantageous for reducing costs and milling time.

## 6.1 Mechanism Involved

- Real comminution: the primary particles are ground during a liquid phase by high shearing, pressure, and impact forces.
- De-agglomeration and dispersing: agglomerates are dispersed by high shearing, pressure, and impact forces. The surface air is removed and the surface of the particle is easily wetted (Fig. 3.7).

The fracturing of a particle can occur when the force exceeds the elastic limit of the particles. Different theories of size reduction are involved (Table 3.1).

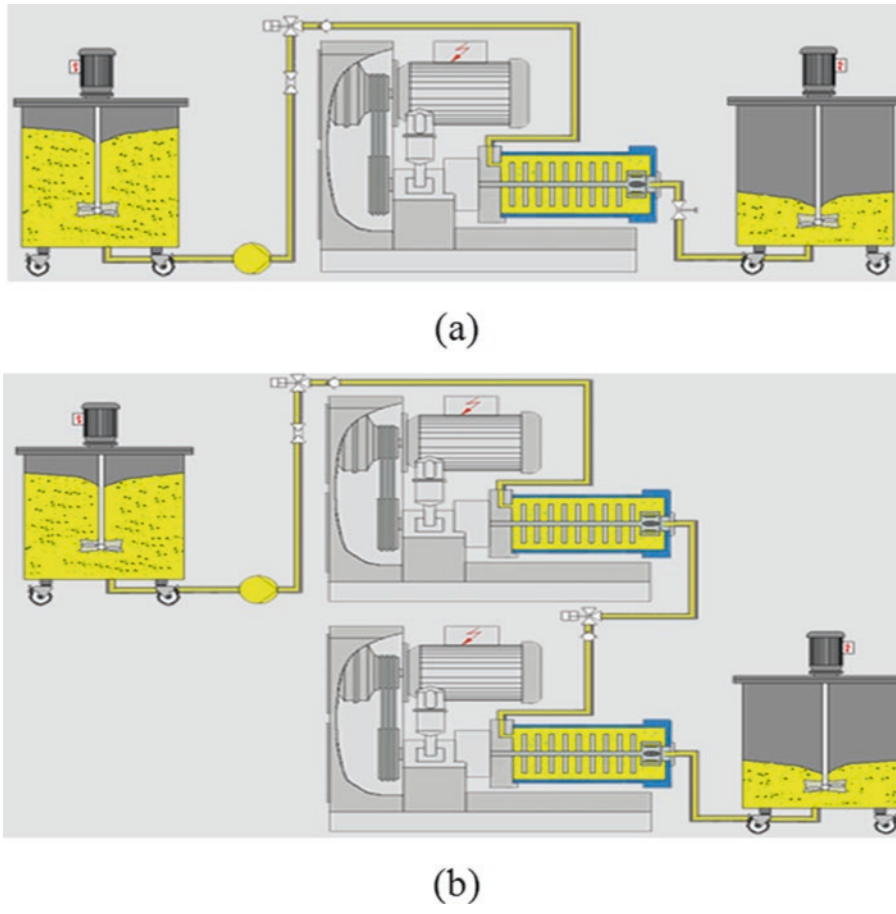


**Fig. 3.6** Batch wet bead milling process with (**a**) one or (**b**) more milling chambers

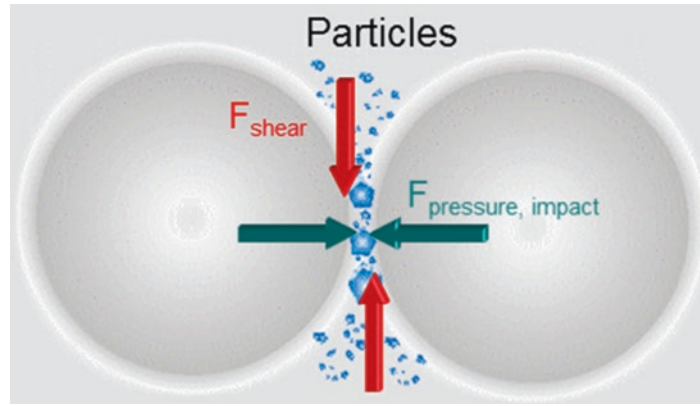


**Fig. 3.7** Mechanism involved in the bead milling process

**Table 3.1** Different theories of size reduction

| Theory | Principle |
|---|---|
| Griffith theory | The amount of force to be applied, which depends on the length of the crack and the focus of stress at the atomic bond of the apex of the crack |
| Kick's law | Work required to reduce the size of a given quantity of material is constant for the same reduction ratio regardless of the original size |
| Rittinger's law | Work useful to reduce particle size is directly proportional to the new particle surface area produced |
| Bond's law | Work useful to reduce particle size is proportional to the square root of the diameter of the particle produced |

## 6.2 Selection of Bead Size

The bead diameter is limited by its relationship to the particles. The particles should be smaller than the void volume between the grinding beads. Generally, the selection of bead size depends on the following practical rules, which can form the basis of reference points:

- Diameter of the grinding media should be approximately 20–50 times larger than the $d_{99}$ of the particle.
- 1/1,000 diameter value of the selected grinding media is the $d_{50}$ of the final particle size.

Selection of the grinding media depends on the grinding characteristics of the particles, which have to be considered (such as hardness, grain shape, agglomerate/primary grain) to determine the best bead size. Different types of grinding media are available on the market (Table 3.2). Selection of the media type is done based on the criticality of milling process and the formulation requirements. The design of the bead separation system must be suitable for the size of the beads and the feed material size. The screen opening should be from one-third to one-half the diameter of the beads. Thus, overall, the bead milling process depends on the different parameters such as formulation, percentage solids, additives, vehicle, viscosity, mixer speed, flow rate, inlet pressure, outlet temperature, shaft speed, screen size, cooling water temperature and flow, motor power, bead density, bead size, and bead filling.

Currently, pharmaceutical milling machines are designed and built in accordance with the cGMP (Current Good Manufacturing Practices of the Food and Drug Administration), GAMP (Good Automated Manufacturing Practices), GAMP5, ASME BPE (Bioprocessing Equipment Standard of American Society of Mechanical Engineers). UL or CE Electrical components, 21 CFR Part 11 Compliance, FDA (Food and Drug Administration) guidelines or meeting the specifications of other regulatory bodies.

The major disadvantage of this technology includes high energy leading to stability concerns regarding the drugs, contamination from the milling media, and time consumption, as a long-term operation ranging from hours to days is generally required. The long-term operation is dependent on the properties of the drug, the milling media, and the extent of particle size reduction (Gao et al. 2008; Peltonen and Hirvonen 2010). To overcome the above constraints to a certain extent, coolant is circulated to reduce the thermogenic effect. For long-term operation, it is also recommended to use special Yttrium Stabilized Zirconia (YSZ) grinding beads, which have the following special features/advantages:

- Highly cost-effective, low wear, and a long lifetime: YSZ milling/grinding material is the most durable and efficient medium for ball milling of ceramic materials. It reduces operational costs because of its ultra-low wear.
- Relatively high mechanical strength, beads do not break owing to toughness and impact resistance performance.
- High specific gravity, high efficiency, which saves processing time.
- Very smooth and extremely well-polished, even easy to clean, low abrasion to the internal wall of equipment.
- Highly resistant to acids and solvents.
- Because it is virtually contamination free it is an ideal solution for a variety of applications that demand minimal contamination, including, but

**Table 3.2** Different types of grinding media

| Grinding media type | Density (kg/dm$^3$) | Minimum diameter $d_{min}$ (mm) | Relative wear rate |
|---|---|---|---|
| Plastic | 0.9–2.1 | ≥ 0.15 | + |
| Glass | 2.5 | ≥ 0.05 | 0 |
| Quartz sand | 2.65 | ≥ 0.1 | −0 |
| Ottawa sand | 2.65 | ≥ 0.2 | 0 + |
| $Al_2O_3$ (99.7%) | 3.2 | ≥ 0.4 | 0 |
| $Al_2O_3$ (99.9%) | 3.2 | ≥ 1.0 | ++ |
| Zirconium silicate | 3.7–3.8 | ≥ 0.2 | 0 + |
| $Al_2O_3/ZrO_2$ | 4.1 | ≥ 0.6 | + |
| $ZrO_2/Y_2O_3$/zirconium silicate | 4.6 | ≥ 0.2 | + |
| $ZrO_2$/MgO – stabilized | 5.5 | ≥ 0.4 | – |
| $ZrO_2/Y_2O_3$ – stabilized | 6 | ≥ 0.05 | ++ |
| $ZrO_2$/CeO – stabilized | 6.1–6.2 | ≥ 0.4 | + |
| Steel shot | 7 | ≥ 0.1 | 0 |
| Steel | 7.75 | ≥ 1.0 | 0 + |
| Quality increased → | | | |
| -- - 0 + ++ | | | |

not limited to, nanomaterials, pharmaceuticals, foods, chemicals, batteries, inks, toner, dielectrics, solar cells, semiconductors, aluminum nanoparticles, etc. (Rijesh et al. 2018).

The wet milling approaches of crystalline nanosuspensions in the pharmaceutical industry can also be judged by the fact that more than 20 formulations are already on the market and close to 15 are at different stages of clinical trials (Table 3.3). The modern and sterile wet milling process is a widely adopted processing technology by the pharmaceutical industry for developing different commercial products (Kumar and Burgess 2012; Gulsun et al. 2009; Moschwitzer 2013; Junyaprasert and Morakul 2015). Scaling up with a media mill is possible, but there is a certain limitation in media mill chamber size owing to its weight so that to produce a larger batch size the media mills can be configured in the circulation mode or more milling chambers can be attached. Typically, from a small laboratory scale to a larger production scale can be carried out with different sized chambers from 5 to 15 ml to a few liters, which are commercially available from the Nanomill® system (élan Drug Discovery, King of Prussia, PA, USA), Dynomill (Glen Mills, Clifton, NJ, USA), and Netzsch mills (Netzsch, Exton, PA, USA)).

## 6.3 Particle Surface Modification

Many orally administered nanosuspensions are modified on the surface using mucoadhesive polymers such as chitosan and carbomer, which can increase the adhesion to the gut wall. The residence time can be increased by improving the adhesiveness of nanocrystals to lumen in the gastrointestinal tract with the addition of mucoadhesive polymers (Thanki et al. 2013; Müller et al. 2001).

In other examples of ophthalmic nanosuspensions, polymers such as carbomer, hydroxypropyl methyl cellulose (HPMC), polyvinylpyrrolidone (PVP), and polyvinyl alcohol (PVA) were used as suspension agents (Bartos et al. 2018).

In many examples, the addition of stabilizers on the particle surface works as physical stabilizers and they may have additional properties such as modifying their bioavailability and pharmaco-

**Table 3.3** Examples of FDA-approved nanocrystal products

| Drug | Trade name | Dosage form | Manufacturer | Year |
|---|---|---|---|---|
| Dexamethasone; tobramycin | Tobradex | Ophthalmic suspension | Novartis | 1988 |
| Verapamil hydrochloride | Verelan PM® | Capsule | Schwarz Pharma | 1998 |
| Brinzolamide | Azopt® | Ophthalmic suspension | Novartis | 1998 |
| Dexmethylphenidate hydrochloride | Focalin XR® | Capsule | Novartis | 2001 |
| Sirolimus | Rapamune® | Tablet | Wyeth | 2000 |
| Tizanidine hydrochloride | Zanaflex® | Capsule | Acorda | 2002 |
| Morphine sulfate | Avinza® | Capsule | King Pharma | 2002 |
| Methylphenidate hydrochloride | Ritalin LA® | Capsule | Novartis | 2002 |
| Diltiazem | Herbesser® | Tablet | Mitsubishi | 2002 |
| Aprepitant | Emend® | Capsule | Merck | 2003 |
| Dexamethasone; ciprofloxacin | Ciprodex | Ophthalmic suspension | Novartis | 2003 |
| Fenofibrate | Tricor® | Tablet | Abbott | 2004 |
| Fenofibrate | Triglide® | Tablet | Skye Pharma | 2005 |
| Megestrol acetate | Megace® ES | Suspension | Par Pharma | 2005 |
| Megestrol acetate | Megace® ES | Oral suspension | PAR Pharmaceuticals | 2005 |
| Nepafenac | Nevanac | Ophthalmic suspension | Novartis | 2005 |
| Naproxen sodium | Naprelan® | Tablet | Wyeth | 2006 |
| Theophylline | Theodur® | Tablet, capsule | Mitsubishi Tanabe Pharma | 2008 |
| Paliperidone palmitate | Invega Sustenna® | Monthly intramuscular depot injection | Johnson & Johnson | 2009 |
| Nepafenac | Ilevro® | Ophthalmic suspension | Novartis | 2012 |
| Aripiprazole | Abilify Maintena kit® | Intramuscular injection | Otsuka Pharmaceutical Co. Ltd. | 2014 |
| Paliperidone palmitate | Invega Trinza® | Three-monthly intramuscular depot injection | Johnson & Johnson | 2015 |
| Aripiprazole lauroxil | Aristada initio kit® | Intramuscular injection | Alkermes INC | 2018 |

logical activity. For example, albumin, arginine, lecithin, leucin, vitamin E polyethylene glycol succinate (TPGS), and sodium cholic acid provided nanocrystals with additional favorable biological properties.

Coating the nanocrystals with surfactants was done to allow barrier crossing and access to treating brain diseases by modifying the permeation at the blood–brain barrier (BBB). For example, atovaquone was safely and effectively used against *T. gondii* in vitro to treat toxoplasmic encephalitis, but the oral micronized solution showed poor bioavailability. In vivo studies confirmed the capacity of nanosuspensions coated with sodium dodecyl sulfate to cross the blood–brain barrier and permit the treatment of toxoplasmic encephalitis and other cerebral diseases (Shubar et al. 2011).

## 7 Cryo-Milling

### 7.1 Definition

Cryo-milling is a technique that involves high-energy ball milling performed in liquid nitrogen at cryogenic temperatures. Because of the intense ball milling at these temperatures, the size of the original powder is reduced to the nanoscale level in a relatively shorter time. Furthermore, the cryo-milling process is capable of producing nanocrystalline materials with enhanced thermal stability of particles. Thus, among the different mechanical processes, such as inert gas condensation, electrode position, rapid solidification, and sputtering, cryo-milling represents a new and effective technique for the production of nano-sized powders (Birringer et al. 1984; Back et al. 2005).

### 7.2 Ultra Cryo-Milling

An ultra cryo-milling technique uses liquid nitrogen and dry ice as beads. Liquid nitrogen is used as a dispersing solvent instead of water and dry ice was used as a milling medium instead of zirconia beads. The crystals are pulverized by collision with the dry ice beads at cryogenic temperatures. Because dry ice beads and liquid nitrogen spontaneously sublimate and vaporize under ambient conditions, both materials can be easily removed after the milling process, resulting in no residual solvent or bead material remnants in the milled product. Even if beads are broken or eroded during the milling process, there is no concern about contamination. The milled material is easily and efficiently recovered because the separation process from the beads is not necessary. Thus, it is also called a contamination-free cryo-milling technique. It is also advantageous that the dried products are directly available owing to spontaneous vaporization of liquid nitrogen so that a drying process is not required after the process. Thus, this approach encompasses the advantages of both dry and wet milling.

It has been reported that the milling efficiency is much higher than with dry milling using jet milling because dispersing the medium would actively disturb the coaggregation between the milled particles. In contrast, it has also been reported that the milling efficiency is slower compared with the zirconia beads at cryogenic temperatures, suggesting that dry ice is an inferior milling material to zirconia in liquid nitrogen under cryogenic conditions. The mechanism of wet media milling has been reported as the collision between the beads and the vessel wall. The milling efficiency is mainly dependent on collision energy. Heavy zirconia bead density (6.0 g/cm$^3$) would likely provide a higher collision energy to the particles than a light dry ice bead density (1.56 g/cm$^3$). In addition, zirconia beads have a more uniform size, a smoother surface, and a more rigid body than dry ice beads; thus, effective milling power would result from collision between heavier, similar-sized, and smooth-surfaced beads (Uemoto et al. 2018) (Table 3.4).

## 8 Solvent–Antisolvent Precipitation

Antisolvent precipitation is a bottom-up method, and produces fine particles by starting at the atomic level. This method gives better control over particle properties such as size, morphology, and crystallinity, compared with top-down methods. Antisolvent precipitation is the most attractive method of all the bottom-up methods. Antisolvent precipitation techniques provide a more convenient procedure at room temperatures and atmospheric pressure with no specific requirement of expensive equipment, and is at the same time easily scalable compared with other bottom-up methods (Dua et al. 2015).

### 8.1 Fundamental Principle of Antisolvent Precipitation Techniques

Antisolvent precipitation techniques proceed in steps of mixing of the solution and antisolvent, the generation of supersaturation, nucleation, and growth by coagulation and condensation, followed by agglomeration in the case of uncontrolled growth (Fig. 3.8).

The precipitation driving force is speedy and eminent supersaturation. The crucial crystal properties, such as size, morphology, and purity are significantly dependent on the rate, magnitude, and uniformity of supersaturation that generated during the process of crystallization (Mullin and Nyvlt 1971; Jones and Mullin 1974).

One component of the crystals' supersaturation ($S$) in liquids is defined in Eq. (3.3):

$$S = \frac{C}{C*} \tag{3.3}$$

where $C$ is the actual drug concentration in the solution (mol/l) and $C*$ is the drug equilibrium solubility (mol/l) in a mixture of organic solvent and antisolvent.

It has been frequently observed that a higher degree of supersaturation typically results in lower Gibbs free energy and leads to higher nucleation rates (Dirksen and Ring 1991; Sugimoto 2003; Cushing et al. 2004).

**Table 3.4** Examples obtained from the scientific literature on the use of cryo-milling for the production of drug nanoparticles

| Drug | Observations | Equipment | References |
|---|---|---|---|
| Phenytoin | Novel ultra cryo-milling micronization technique using dry ice beads and liquid nitrogen | Wet milling machine (RMB-04, Aimex, Tokyo, Japan) | Sugimoto et al. (2012a, b) |
| Griseofulvin | Continued mode of attrition with milling time | Cryogenic impact mill (Spex CertiPrep 6750, Metuchen, NJ, USA) | Otte and Carvajal (2011) |
| Ketoconazole | Continued milling caused apparent particle growth | | |
| Furosemide | Solid state amorphization and chemical decomposition | Cryogenic impact mill (Spex CertiPrep 6750) | Adrjanowicz et al. (2011) |
| Indomethacin | Dissolution rate depended on the milling time | Oscillatory ball mill (Mixer Mill MM301, Retsch, Haan, Germany) | Karmwar et al. (2011, 2012), Botker et al. (2011) |
| Phenytoin, ibuprofen, salbutamol sulfate | No change in crystal form and amorphization after milling | Wet milling machine (RMB-04, Aimex) | Niwa et al. (2010) |
| Glibenclamide | Transformation from crystalline to amorphous state without chemical decomposition | Cryogenic freezer/mill (Spex SamplePrep 6770) | Wojnarowska et al. (2010) |
| Ranitidine hydrochloride | Ranitidine hydrochloride polymorph forms 1 and 2 could be fully converted to the amorphous form | Oscillatory ball mill (Mixer Mill MM301, Retsch) | Chieng et al. (2008) |
| Carbamazepine | Higher amorphization with cryogenic co-grinding than with room temperature co-grinding | Cryogenic impact mill (Spex CertiPrep 6750) | Jayasankar et al. (2006) |
| Whole inactivated influenza virus | Dry powder influenza vaccine successfully formulated | Micro-ball mill (SPEX CertiPrep 3117) | Garmise et al. (2006) |
| Indomethacin polymorphs and solvates | Amorphous materials obtained after milling possessed similar Tg, but significant differences in their physical stability | Cryogenic impact mill (Spex CertiPrep 6750) | Crowley and Zografi (2002) |

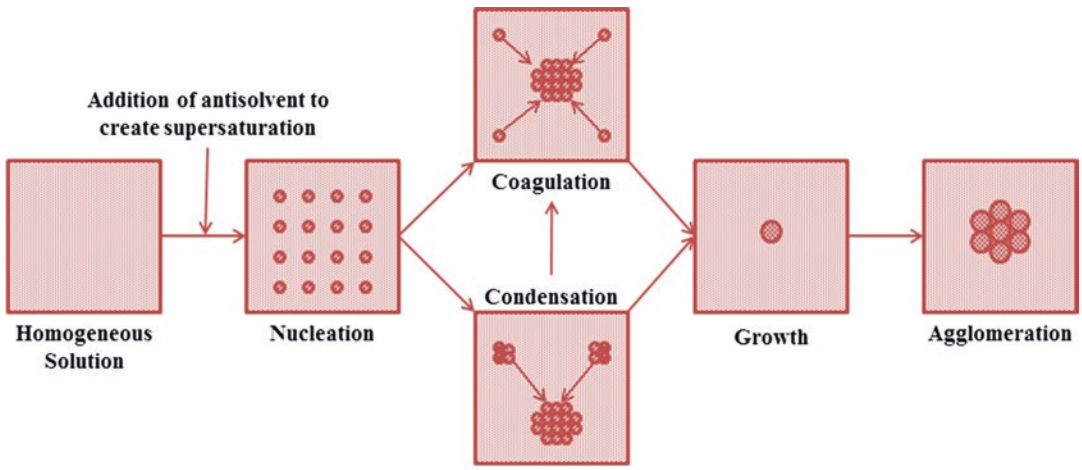


**Fig. 3.8** The particle precipitation process

$$B^0 \propto \exp\left(\frac{\Delta Gcr}{kT}\right) \tag{3.4}$$

where $B^0$ is the nucleation rate, $k$ is Boltzmann's constant, $\Delta Gcr$ is the critical free energy, and $T$ is the absolute temperature.

There are two mechanisms of "primary" nucleation, homogeneous and heterogeneous nucleation. In homogenous nucleation, the new solid phase generation is in the absence of foreign particles and surrounding surfaces. While in heterogeneous nucleation, the existing foreign particles promote nucleation (Söhnel and Garside 1992). In contrast, "secondary nucleation" is started by existing native crystals through mechanical abrasion or through thermodynamic effects.

The free energy for homogeneous nucleation is given in Eq. (3.5):

$$\Delta Gcr = \frac{16\pi\gamma_{sl}^3\upsilon^2}{3(kT)^2\left(\ln(1+s)\right)^2} \tag{3.5}$$

Thus, after combining Eqs. (3.4) and (3.5), the rate of homogeneous nucleation in the solution is derived by (Eq. 3.6)

$$B^0 = A_{\text{hom}} \exp\left(-\frac{16\pi\gamma_{sl}^3\upsilon^2}{3k^3T^3\left(\ln(1+s)\right)^2}\right) \tag{3.6}$$

where $B^0$ is the nucleation rate, $A_{\text{hom}}$ is the pre-exponential factor, $\gamma_{sl}$ is the interfacial tension at the solid–liquid interface, $\upsilon$ is the molar volume, and T is the temperature. Nucleation rates are primarily dependent on supersaturation and interfacial energy ($\gamma$), and the order of magnitude of $A_{\text{hom}}$ typically varies from $10^{32}$ to $10^{36}$. Furthermore, $A_{\text{hom}}$ is dependent on the attachment mechanism of the solute on the growing particle surface, i.e., either interface transfer control or volume diffusion control (Johnson 2003; LaMer and Dinegar 1950; Guo et al. 2005; Matteucci et al. 2006; Dalvi and Dave 2010). Table 3.5 summarizes the various examples of drugs obtained from the scientific literature on the use of the antisolvent precipitation technique.

To obtain nanoparticles with a narrow size distribution, the following parameters should be kept in mind:

- Create a high degree of super saturation
- Uniform spatial concentration distributions in solutions
- Negligible growth of all crystals

There are two important parameters. One is the meta stable zone, the range of concentration where no crystallization is observed within a given time. It also called the energy barrier for particle precipitation from saturated solution. In order to achieve higher nucleation rates, a meta stable zone width should be shorter. Another parameter is the induction time. The induction time is the time elapsed between suspension of supersaturation and the appearance of detectable crystals (Granberg et al. 2001; Dixit and Zukoski 2002; Lyczko et al. 2002; Barrett and Glennon 2002; Omar et al. 2006; Schöll et al. 2007; Lindenberg and Mazzotti 2009; Kelly and Rodr'guez-Hornedo 2009; Mahajan and Kirwan 1993; Kim and Mersmann 2001; Chen et al. 2000; Dalvi and Dave 2009).

The nucleation and growth of particles occur simultaneously and both compete for consumption of supersaturation. Once nucleation occurs, the particles grow by condensation ($\tau_{\text{cond}}$) and by coagulation ($\tau_{\text{coag}}$). Condensation competes with nucleation by decreasing supersaturation. Coagulation can reduce the rate of condensation by reducing the total number of particles and the surface area (Thybo et al. 2008; Sun 2002; Jones 2002).

Once the particles grow, they also start to agglomerate because the process depends on the population density. Further agglomeration also depends on the Brownian motion of nanoparticles. It has been reported that at higher temperatures, the Brownian motion increases and results in a further increase in the growth rates of crystals. While at lower temperatures, the smaller crystals and the larger population density with higher surface energy cause agglomeration (Lince et al. 2008).

**Table 3.5** Examples of various drug nanoparticles by antisolvent precipitation

| Drug | Water solubility (mg/ml) | Nucleation type/model | Particle size (nm) | References |
|---|---|---|---|---|
| Alpha ketoglutarate | – | – | 110 | Sultana et al. (2011) |
| Ascorbyl palmitate | 0.34 | Classical theory of homogeneous nucleation | 780 | Beck et al. (2010) |
| Atropine sulfate | 2.2 | – | 100–600 | Ali et al. (2009a) |
| Atorvastatin calcium | 0.12 | – | 240 | Zhang et al. (2009a) |
| Beclomethasone dipropionate | 0.049 | Classical theory of homogeneous nucleation | 440 | |
| Bicalutamide | 0.005 | Classical theory of nucleation with some modification | 115 | Lindfors et al. (2008) |
| β-Carotene | – | Primary nucleation | 100 | Zhu et al. (2007) |
| β-Carotene and $C_{12}$-Au | – | – | 103 | Gindy et al. (2008a) |
| Cefuroxime axetil | 0.145 | Primary nucleation | 80 | Dhumal et al. (2008a) |
| Cefradine | 21.3 | Homogeneous nucleation | 300 | Zhong et al. (2005) |
| Curcumin | 0.00019 | Nonclassical pathway | 30–50 | He et al. (2010, 2011) |
| Danazol | 0.238 | Homogeneous nucleation | 364 | Zhao et al. (2007) |
| Danazol | 0.238 | Homogeneous nucleation | 190 | Zhao et al. (2009) |
| Diatrizoic acid | 0.39 | – | 136 | El-Gendy et al. (2010) |
| Docetaxel | 0.000025 | – | 180 | Cheng et al. (2007a) |
| Felodipine | 0.356 | – | 60 | Lindfors et al. (2007) |
| Fenofibrate | 0.25 | Classical theory of homogeneous nucleation | 882 | Meng et al. (2009) |
| Hydrocortisone | 0.32 | – | 80 | Ali et al. (2009b) |
| Ibuprofen | 0.049 | Classical theory of homogeneous nucleation | 702 | Dalvi and Dave (2010) |
| Insulin | – | – | 200 | Klingler et al. (2009) |
| Itraconazole | Insoluble | Homogeneous primary nucleation | 300 | Matteucci et al. (2006, 2008) |
| Maleimide | – | – | 85 | Gindy et al. (2008b) |
| Megestrol acetate | 0.002 | Classical theory of homogeneous nucleation | 208 | Zhang et al. (2009b) |
| Nitrendipine | 0.19 | Classical theory of homogeneous nucleation | 209 | Xia et al. (2010) |
| Norfloxacin | 0.264 | – | 170 | Panagiotou et al. (2009) |
| Odanacatib | – | Classical theory of homogeneous nucleation | 350 | Kumar et al. (2009a) |
| Paclitaxel | 0.277 | – | 100 | Pattekari et al. (2011) |
| PLGA and PLA | – | – | 84–168 | Bilati et al. (2005) |
| PLGA-PEG and PLGA-lipid | – | – | 70–80 | Valencia et al. (2010) |
| Progesterone | 0.00881 | – | 267 | Salem (2010) |

(continued)

**Table 3.5** (continued)

| Drug | Water solubility (mg/ml) | Nucleation type/model | Particle size (nm) | References |
|---|---|---|---|---|
| Roxithromycin | 0.0000189 | Classical theory of homogeneous nucleation | – | Guo (2005) |
| Salbutamol sulfate | 0.003 | Classical theory of homogeneous nucleation | 100 | Hu et al. (2008) |
| Salmeterol xinafoate | 0.11 | Classical theory of homogeneous nucleation | 254 | Murnane et al. (2008) |
| Sirolimus | 0.086 | Classical theory of homogeneous nucleation | 863 | Gandhi and Murthy (2010) |
| Spironolactone | 0.022 | A spherical cluster was formed first, followed by rearrangement of the spheres into ordered nanocrystals | 330 | Dong et al. (2011), Erdemir et al. 2009) |
| Theophylline | 5 | – | 290 | Salem et al. (2011a) |

*PEG* poly(ethylene glycol), P*LGA* poly(lactide-coglycolide), *PLA* polylactic acid

Particle engineering requires the fine-tuning of different variables such as meta stable zone width, induction time, interfacial surface energy, and supersaturation, to obtain the desired particle characteristics. However, fine tuning and control of these variables require prior observations and in situ measurements. Several methods have been reported for the detection and measurement of nucleation and growth kinetics so far and are summarized in Table 3.6.

## 8.2 Step-Up Antisolvent Precipitation Process

### 8.2.1 Mixing

Mixing generates supersaturation followed by nucleation and growth in a step-up antisolvent precipitation process. There are two main time scales, mixing time ($\tau_{mix}$) and the precipitation or induction time ($\tau_{precipitation}$), both of which are associated with the process of particle formation. Mixing time ($\tau_{mix}$) comprises the time required for macro mixing, meso mixing, and micro mixing. Mixing that occurs on a crystallizer scale is called macro mixing. Meso mixing is also known as turbulent mixing and it consists of the large-scale mass transfer of a solution. Molecular diffusion and engulfment of different solvent composition regions below the Kolmogorov micro scale is called micro mixing (Johnson and Prud'homme 2003a, b; Gradl et al. 2006; Shekunov et al. 2001; Baldyga et al. 1997). $\tau_{precipitation}$ is composed of nucleation time ($\tau_{nucleation}$) and growth time ($\tau_{growth}$). The Damköhler number (Da), dimensionless is the ratio of $\tau_{mix}$ to $\tau_{precipitation}$. Thus, when Da is greater than 1, the mixing process is slower than the precipitation process, supersaturation is accomplished at a slower rate, and the metastable zone is crossed very slowly. This leads to particle growth and the formation of large crystals. On the other hand, when Da is less than 1, $\tau_{mix}$ is reduced compared with $\tau_{precipitation}$, the solution is mixed uniformly at the micro level, where supersaturation is accomplished rapidly and nucleation takes place swiftly. The mixing process is faster than the precipitation step and controls overall particle formation. In a situation where supersaturation is highly accomplished, then the meta stable zone is crossed quickly, and nucleation dominates in the precipitation process. This leads to a large number of nuclei and the precipitation of nanoparticles with a narrower size distribution.

Currently, two approaches have been reportedly used for increasing the mixing rate; namely, the high jet velocity mixing device and ultrasound precipitation (Muntó et al. 2005; Zhao et al. 2007; Beck et al. 2010).

### 8.2.2 Mixing Devices

There are various mixing device designs reported, such as a static mixer, high gravity precipitation, a confined impinging jet, a multi-inlet vortex

**Table 3.6** Methods for the detection and measurement of nucleation and growth kinetics

| Purpose | Characterization techniques | References |
|---|---|---|
| Nucleation and growth kinetics | ATR-FTIR | Schöll et al. (2007) |
| | FBRM | Barrett and Glennon (2002, Schöll et al. (2007) |
| | Laminar flow diffusion chamber | Dong et al. (2011) |
| | Raman spectroscopy | Ali et al. (2011) |
| | Microscopic analysis | Zhu et al. (2010b) |
| Metastable zone width | FBRM | Barrett and Glennon (2002) |
| | Saturation temperature measurement | Lyczko et al. (2002) |
| | Visual appearance | Liu et al. (2010b) |
| Induction time | FBRM | Barrett and Glennon (2002), Lindenberg and Mazzotti (2009) |
| | ATR-FTIR | Schöll et al. (2007), Lindenberg and Mazzotti (2009) |
| | Visual appearance | Omar et al. (2006) |
| | Laser scattering method | Zhi et al. (2011) |
| | Conductivity measurement | Lyczko et al. (2002) |
| | Lasentec PVM | Omar et al. (2006) |
| | SEM | Teychene and Biscans (2008) |
| Interfacial energy | Theoretical correlation by Mersmann and Bennema | Teychene and Biscans (2008) |
| | Contact angle measurement using KVS CAM 200 equipped with a CCD camera | |
| | Contact angle measurement using Young equation | Granberg et al. (2001) |
| | Using tensiometer: (Krüss processor tensiometer K12, Wilhelmy plate method) | |

(continued)

**Table 3.6** (continued)

*ATR-FTIR* attenuated total reflection-Fourier transform infrared spectroscopy, *CCD* charge-coupled device, *FBRM* focused beam reflectance measurement, *PVM* particle vision and measurement, *SEM* scanning electron microscopy

mixer (MIVM), a Y-shaped micro channel reactor, and a T-mixer.

Mixing devices facilitate the process and intensify nanoparticle formation by reducing the diffusion length between drugs containing a solvent and those containing an antisolvent. Mixing devices help to achieve mixing time by milli- to microseconds. In some mixer designs, additional ultrasound as an external energy can help in rapid mixing to achieve higher supersaturation in a very short time.

A *static mixer* consists of a series of motionless identical elements with a specific structure of mixing elements. The mixing elements are able to redistribute fluid in the radial and tangential directions to realize rapid and homogeneous mixing. Many of the research groups reported the use of static mixing for antisolvent precipitation of drug nanoparticles, as summarized in Table 3.7 (Gassmann et al. 1994; Douroumis and Fahr 2006; Douroumis et al. 2008; Dong et al. 2010; Hu et al. 2011).

*High gravity antisolvent precipitation (HGAP)*, where, under the high gravity, the rotating packed bed disseminates or breaks up the fluids into very fine droplets. The rate of mass transfer is higher in a rotating packed bed than in a conventional reactor. The particle size decreases as the rotating speed is increased. The use of HGAP in the production of fine particles of danazol, cefuroxime axetil, salbutamol sulfate, and cefradine has been reported (Hu et al. 2008; Zhao et al. 2009; Chiou et al. 2007; Zhong et al. 2005; Chen et al. 2006).

A *multi-inlet vortex mixer* has been reported for many organic and inorganic compounds via flash nanoprecipitation, as summarized in Table 3.7, where the mixing rate is too rapid and requires less time compared with nucleation and drug particle growth time. The flow rate can be adjustable with the entry of solvent and antisolvent into the mixer in such a way that different levels of supersatura-

**Table 3.7** Summary of mixing devices used for the antisolvent precipitation technique

| Process | Drug | Particle size (nm) | References |
|---|---|---|---|
| Static mixer | Betamethasone valerate-17 | 250 | Douroumis and Fahr (2006) |
| | Oxcarbazepine | 970 | |
| | Spironolactone | 500 | Dong et al. (2010) |
| | Fenofibrate | 328 | Hu et al. (2011) |
| HGRP | Benzoic acid by reacting sodium benzoate and HCl | 10 | Chen et al. (2004) |
| | Cefradine | 300 | Zhong et al. (2005) |
| | Competitive boric acid, iodate, and iodide reaction | – | Yang et al. (2005) |
| | Cefuroxime axetil | 305 | Chen et al. (2006) |
| | Danazol | 190 | Zhao et al. (2009) |
| CIJ | Competitive Bourne reactions | – | Johnson and Prud'homme (2003a) |
| | β-Carotene | 100 | Johnson and Prud'homme (2003b) |
| | Cyclosporine A | 18–700 | Chiou et al. (2008) |
| | Competitive iodide–iodate model reaction | 300 | Hu et al. (2008) |
| | Poly-ε-caprolactone and poly(methoxypolyethyleneglycol cyanoacrylate-co-hexadecyl cyanoacrylate) | 150 | Lince et al. (2011) |
| Impinging device | Spironolactone | 302 | Dong et al. (2011) |
| Multi-inlet vortex mixer | Competitive Bourne reactions | – | Liu et al. (2008) |
| | β-Carotene and $C_{12}$-Au | 103 | Gindy et al. (2008a) |
| | Maleimide | 85 | Gindy et al. (2008c) |
| | β-Carotene | 100 | Zhu et al. (2010a) |
| Mixing tee with ultrasound | Itraconazole | 145 | Cheng et al. (2009) |
| | Odanacatib | 350 | |
| YMCR | Danazol | 364 | Zhao et al. (2007) |
| | Hydrocortisone | 295 | Ali et al. (2011) |
| | Atorvastatin calcium | 480 | Zhang et al. (2010) |
| | Cefuroxime axetil | 350 | Wang et al. (2010) |
| Microporous tube-in-tube microchannel reactor | Cefuroxime axetil | 400 | Zhu et al. (2010b) |
| T-shaped microchannel | Curcumin | 190 | (Liu et al. 2010b) |
| T-mixer with ultrasound | Ascorbyl palmitate | 780 | Beck et al. (2010) |
| | Itraconazole | 347 | |
| Ultrasound with batch reactor | Cefuroxime axetil | 80 | Dhumal et al. (2008b) |
| | Ibuprofen | 702 | Verma et al. (2009) |
| | Curcumin | 60 | Zheng et al. (2010) |
| | Diatrizoic acid | 136 | El-Gendy et al. (2010) |
| | Nitrendipine | 209 | Xia et al. (2010) |
| | Sirolimus | 863 | Gandhi and Murthy (2010) |

*CIJ* confined impinging jet, *HGRP* high-gravity reactive precipitation, *YMCR* Y-shaped microfluidic reactor

tion can be achievable. An adjustable facility can help to control the adsorption of the stabilizer, particle growth, and the size of the nanoparticles. Based on the literature, it has been observed that the end fluid phase, which contains mostly antisolvent and a smaller amount of organic solvent in the

end solution helps to reduce the extent of Ostwald ripening of particle suspensions (Liu et al. 2007, 2008; Gindy et al. 2008c, d; Kumar et al. 2009b; Zhu et al. 2010a; Cheng et al. 2009).

A *confined impinging jet (CIJ)* is reported for the nanoparticle production of several drugs via the antisolvent precipitation technique. The high velocity jet of fluid facilitates the rapid mixing, ensuring a shorter mixing time than precipitation. The CIJ reactor chamber's geometry, size, and ratio of chamber diameter to jet diameter impact the mixing performance. This high mixing efficiency assists in achieving high supersaturation and high nucleation results in uniform fine nanoparticle precipitation. Furthermore, fast stabilizer distribution on the newly formed surfaces of the nanoparticles via adjustment of the precipitation kinetics of the stabilizer and the drug results in very fine and uniformly stabilized drug nanoparticles (Mahajan and Kirwan 1996; Chiou et al. 2008).

*Microchannel reactor technology (MRT)* provides a high level of velocity and energy dissipation compared with a conventional reactor. Microreactor mixing is mainly operated by molecular diffusion. Moreover, fine control of supersaturation can be achieved by proper selection of stream ratios. MRT is a continuous process and scalable to enable handling of flow rates of a few liters per minute. There are different shaped micro channel reactors reported in the literature. Y-shaped mixers have been used for the precipitation of danazol, hydrocortisone, atorvastatin calcium, and cefuroxime axetil nanoparticles. Similarly, the reported T-mixers remove the issues of proper alignment of nozzles associated with impinging jets. T-mixers are also used in combination with ultrasound in antisolvent precipitations such as fenofibrate, itraconazole, griseofulvin, ascorbyl palmitate, and sulfamethoxazole. Ultrasound used in the mixing zone helps to improve mixing and generates high supersaturation, resulting in controlled growth of fine and uniform nanoparticles (Ehrfeld et al. 1999; Panagiotou et al. 2009; Wang et al. 2010; Zhang et al. 2010; Wong et al. 2004).

*Microporous tube-in-tube microchannel reactors (MTMCR)* have provided effective micro mixing and high throughput capacities. It has been reported for use in continuous nanoparticle production of amorphous cefuroxime axetil (Wang et al. 2009).

## 9 Role of Stabilizer in Antisolvent Precipitation Techniques

The role of a stabilizer to make a protective layer on the particle surface during antisolvent precipitation leads to controlled growth and agglomeration. It can be added in either the solvent or the antisolvent phase. There are two main mechanisms of thermodynamic stabilization involved, i.e., steric stabilization and electrostatic repulsion. A list of stabilizers used in the stabilization of nanoparticles during antisolvent precipitation techniques is given in Table 3.8.

## 10 Future Perspectives

The potential of nanocrystals for different applications needed to be investigated in detail. Nanocrystals will combine with implantable sustained release drug delivery systems to attain a higher local concentration. Future perspective studies on novel unique approaches to manufacturing nanocrystals and related products have a huge market. The use of emerging nanocrystal technology is expected to increase in the future, with exploration of different routes of administrations (i.e., oral, parenteral, pulmonary, ocular, and dermal) to enhance

**Table 3.8** Summary of stabilizers for the stabilization of nanoparticles precipitated by antisolvent precipitation techniques

| Drug | Stabilizer | Particle size (nm) | References |
|---|---|---|---|
| Ascorbyl palmitate | PEG (4000) | 780 | Beck et al. (2010) |
| Alpha ketoglutarate | Lutrol F68 and PVA | 110 | Sultana et al. (2011) |
| AC | HPMC | 240 | Zhang et al. (2009a) |
| AZ68 | PVP and SDS, Miglyol | 152 | Sigfridsson et al. (2007) |
| β-Carotene and C12-Au | Poly(ethylene glycol-block-caprolactone) PEG-b-PCL | 103 | Gindy et al. (2008a) |
| β-Carotene | Polycaprolactone | 100 | Zhu et al. (2007) |
| | PS-b-PEO | 100 | Liu et al. (2007) |
| | PEI and chitosan | 60 | Zhu et al. (2010a) |
| | PEG-b-PLGA + poly(acrylic) acid | 140 | Kelly and Rodr'guez-Hornedo (2009) |
| Bicalutamide | Lactose | 330 | Li et al. (2011) |
| | PVP | 115 | Lindfors et al. (2008) |
| Curcumin | PLGA–PEG and Pluronic F-68 | 81 | Anand et al. (2010) |
| | PS and BSA | 60–100 | Yen et al. (2010) |
| | Polyvinyl pyrrolidone | 142 | |
| Cytarabine | PLGA | 125 | Yadav and Sawant (2010) |
| Docetaxel | PLGA-b-PEG | 70 | Cheng et al. (2007b) |
| Fenofibrate | PEG (4000) | 882 | Beck et al. (2010) |
| | SDS and HPMC E3 | 318 | Hu et al. (2011) |
| Hydrocortisone | HPMC, SLS, PVP | 80 | Ali et al. (2009b) |
| | HPMC, PVP, Tween 80 | 295 | Chiou et al. (2008) |
| Itraconazole | Poloxamer 407 | 300 | Matteucci et al. (2006) |
| | HPMC | 300 | Matteucci et al. (2008) |
| | HPMC | 279 | Chen et al. (2008) |
| | Polystyrene-block-polyethylene oxide | 145 | Kumar et al. (2009a) |
| | PEG (4000) | 347 | Beck et al. (2010) |
| Megestrol acetate | PVP and SDS | 208 | Granberg et al. (2001) |
| Nitrendipine | PVA | 209 | Dua et al. (2015) |
| Odanacatib | Polystyrene-block-polyethylene oxide | 350 | Kumar et al. (2009a) |
| Paclitaxel | l-Leucine (Leu) and polyvinylpyrrolidone (PVP K90) | 299 | El-Gendy et al. (2010) |
| | Chitosan and alginic acid | 100 | Pattekari et al. (2011) |
| Progesterone | Stearic acid | 267 | Salem (2010) |
| Sirolimus | Tween-80 | 863 | Gandhi and Murthy (2010) |
| Spironolactone | HPMC | 231 | Dong et al. (2009) |
| | HPMC and SDS | 500 | Dong et al. (2010) |
| | HPMC and SDS | 330 | Zhao et al. (2007) |
| Theophylline | Stearic acid | 290 | Salem et al. (2011b) |

*AC* atorvastatin calcium, *BSA* bovine serum albumin, *HPMC* hydroxypropyl methylcellulose, *PEG* poly(ethylene glycol), *PEG-b-PLGA* poly-(ethylene glycol)-b-poly(lactide-coglycolide), *PEI*, poly(ethylene imine), *PLGA* poly(lactide-coglycolide), *PS* protamine sulfate, *PS-b-PEO* poly(styrene)-b-poly(ethylene oxide), *PVA* polyvinyl alcohol, *PVP* polyvinylpyrrolidone, *SDS* sodium dodecyl sulfate

the bioavailability of nutraceuticals or cosmetics products as well as pharmaceutical products.

## References


Adrjanowicz K, Kaminski K, Grzybowska K, Hawelek L, Paluch M, Gruszka I, Zakowiecki D, Sawicki W, Lepek P, Kamysz W, Guzik L. Effect of cryogrinding on chemical stability of the sparingly water-soluble drug furosemide. Pharm Res. 2011;28(12):3220–36.

Ali R, Jain G, Iqbal Z, Talegaonkar S, Pandit P, Sule S, Malhotra G, Khar R, Bhatnagar A, Ahmad F. Development and clinical trial of nano-atropine sulfate dry powder inhaler as a novel organophosphorous poisoning antidote. Nanomedicine. 2009a;5:55–63.

Ali H, York P, Blagden N. Preparation of hydrocortisone nanosuspension through a bottom-up nanoprecipitation technique using microfluidic reactors. Int J Pharm. 2009b;375:107–13.

Ali H, York P, Ali A, Blagden N. Hydrocortisone nanosuspensions for ophthalmic delivery: a comparative study between microfluidic nanoprecipitation and wet milling. J Control Release. 2011;149:175–81.

Alshora DH, Ibrahim MA, Alanazi FK. Chapter 6 – nanotechnology from particle size reduction to enhancing aqueous solubility. In: Surface chemistry of nanobiomaterials: applications of nanobiomaterials, vol. 3. Cambridge, MA: Elsevier; 2016. p. 163–91.

Anand P, Nair H, Sung B, Kunnumakkara A, Yadav V, Tekmal R, Aggarwal B. Design of curcumin-loaded PLGA nanoparticles formulation with enhanced cellular uptake, and increased bioactivity in vitro and superior bioavailability in vivo. Biochem Pharmacol. 2010;79:330–8.

Baba K, Pudavar HE, Roy I, Ohulchanskyy TY, Chen Y, Pandey RK, Prasad PN. New method for delivering a hydrophobic drug for photodynamic therapy using pure nanocrystal form of the drug. Mol Pharm. 2007;4:289–97.

Back SH, Lee GH, Kang S. Effect of cryomilling on particle size and microstrain in a WC-Co alloy. Mater Trans. 2005;46(1):105–10.

Baldyga J, Bourne J, Hearn S. Interaction between chemical reactions and mixing on various scales. Chem Eng Sci. 1997;52:457–66.

Barrett P, Glennon B. Characterizing the metastable zone width and solubility curve using Lasentec FBRM and PVM. Chem Eng Res Des. 2002;80:799–805.

Bartos C, Jójárt-Laczkovich O, Katona G, Budai-Szűcs M, Ambrus R, Bocsik A, Gróf I, Anna Deli M, Szabó-Révész P. Optimization of a combined wet milling process in order to produce poly(vinyl alcohol) stabilized nanosuspension. Drug Des Devel Ther. 2018;12:1567–80.

Beck C, Dalvi S, Dave R. Controlled liquid antisolvent precipitation using a rapid mixing device. Chem Eng Sci. 2010;65:5669–75.

Bilati U, Allémann E, Doelker E. Development of a nanoprecipitation method intended for the entrapment of hydrophilic drugs into nanoparticles. Eur J Pharm Sci. 2005;24:67–75.

Birringer R, Gleiter H, Klein HP, Marquardt P. Nanocrystalline materials – an approach to a novel solid structure with gas-like disorder? Phys Lett A. 1984;102(8):365–9.

Borchard G. Drug nanocrystals. In: Crommelin D, de Vlieger J, editors. Non-biological complex drugs, AAPS advances in the pharmaceutical sciences series, vol. 20. Cham: Springer; 2015. p. 171–89.

Botker JP, Karmwar P, Strachan CJ, Cornett C, Tian F, Zujovic Z, Rantanen J, Rades T. Assessment of crystalline disorder in cryo-milled samples of indomethacin using atomic pair-wise distribution functions. Int J Pharm. 2011;417(1–2):112–9.

Brouwers J, Tack J, Augustijns P. In vitro behavior of a phosphate ester prodrug of amprenavir in human intestinal fluids and in the Caco-2 system: illustration of intraluminal supersaturation. Int J Pharm. 2007;336:302–9.

Brouwers J, Brewster ME, Augustijns P. Supersaturating drug delivery systems: the answer to solubility-limited oral bioavailability? J Pharm Sci. 2009;98:2549–72.

Chen J, Wang Y, Guo F, Wang X, Zheng C. Synthesis of nanoparticles with novel technology: high-gravity reactive precipitation. Ind Eng Chem Res. 2000;39:948–54.

Chen J, Zhou M, Shao L, Wang Y, Yun J, Chew N, Chan H. Feasibility of preparing nanodrugs by high-gravity reactive precipitation. Int J Pharm. 2004;269:267–74.

Chen J, Zhang J, Shen Z, Zhong J, Yun J. Preparation and characterization of amorphous cefuroxime axetil drug nanoparticles with novel technology: high-gravity antisolvent precipitation. Ind Eng Chem Res. 2006;45:8723–7.

Chen W, Gu B, Wang H, Pan J, Lu W, Hou H. Development and evaluation of novel itraconazole-loaded intravenous nanoparticles. Int J Pharm. 2008;362:133–40.

Chen L, Wang Y, Zhang J, Hao L, Guo H, Lou H, Zhang D. Bexarotene nanocrystal – oral and parenteral formulation development, characterization and pharmacokinetic evaluation. Eur J Pharm Biopharm. 2014;87:160–9.

Cheng J, Teply B, Sherifi I, Sung J, Luther G, Gu F, Levy-Nissenbaum E, Radovic-Moreno A, Langer R, Farokhzad O. Formulation of functionalized PLGA-PEG nanoparticles for in vivo targeted drug delivery. Biomaterials. 2007a;28:869–76.

Cheng J, Teply B, Sherifi I, Sung J, Luther G, Gu F, Nissenbaum E, Radovic-Moreno A, Langer R, Farokhzad O. Formulation of functionalized PLGA-PEG nanoparticles for in vivo targeted drug delivery. Biomaterials. 2007b;28:869–76.

Cheng J, Olsen M, Fox R. A microscale multi-inlet vortex nanoprecipitation reactor: turbulence measurement and simulation. App Phys Lett. 2009;94:204104.

Chieng N, Rades T, Saville D. Formation and physical stability of the amorphous phase of ranitidine hydrochloride polymorphs prepared by cryo-milling. Eur J Pharm Biopharm. 2008;68(3):771–80.

Chiou H, Li L, Hu T, Chan H, Chen J, Yun J. Production of salbutamol sulfate for inhalation by high-gravity controlled antisolvent precipitation. Int J Pharm. 2007;331:93–8.

Chiou H, Chan H, Heng D, Prud'homme R, Raper J. A novel production method for inhalable cyclosporine A powders by confined liquid impinging jet precipitation. J Aerosol Sci. 2008;39:500–9.

Colombo M, Staufenbiel S, Rühl E, Bodmeier R. In situ determination of the saturation solubility of nanocrystals of poorly soluble drugs for dermal application. Int J Pharm. 2017;521:156–66.

Crowley KJ, Zografi G. Cryogenic grinding of indomethacin polymorphs and solvates: assessment of amorphous phase formation and amorphous phase physical stability. J Pharm Sci. 2002;91(2):492–507.

Cushing B, Kolesnichenko V, O'Connor C. Recent advances in the liquid-phase syntheses of inorganic nanoparticles. Chem Rev. 2004;104:3893–946.

Dalvi S, Dave R. Analysis of nucleation kinetics of poorly water-soluble drugs in presence of ultrasound and hydroxypropyl methyl cellulose during antisolvent precipitation. Int J Pharm. 2010;387:172–9.

Dalvi SV, Dave RN. Controlling particle size of a poorly water-soluble drug using ultrasound and stabilizers in antisolvent precipitation. Ind Eng Chem Res. 2009;48:7581–93.

Dhumal R, Biradar S, Yamamura S, Paradkar A, York P. Preparation of amorphous cefuroxime axetil nanoparticles by sonoprecipitation for enhancement of bioavailability. Eur J Pharma Biopharma. 2008a;70:109–15.

Dhumal R, Biradar S, Yamamura S, Paradkar A, York P. Preparation of amorphous cefuroxime axetil nanoparticles by sonoprecipitation for enhancement of bioavailability. Eur J Pharm Biopharm. 2008b;70:109–15.

Dirksen J, Ring T. Fundamentals of crystallization: kinetic effects on particle size distributions and morphology. Chem Eng Sci. 1991;46:2389–427.

Dixit N, Zukoski C. Nucleation rates and induction times during colloidal crystallization: links between models and experiments. Phys Rev. 2002;66:051602.

Dong Y, Ng W, Shen S, Kim S, Tan R. Preparation and characterization of spironolactone nanoparticles by antisolvent precipitation. Int J Pharm. 2009;375:84–8.

Dong Y, Ng W, Hu J, Shen S, Tan R. A continuous and highly effective static mixing process for antisolvent precipitation of nanoparticles of poorly water-soluble drugs. Int J Pharm. 2010;386:256–61.

Dong Y, Ng W, Shen S, Kim S, Tan R. Controlled antisolvent precipitation of spironolactone nanoparticles by impingement mixing. Int J Pharm. 2011;410:175–9.

Douroumis D, Fahr A. Nano- and micro-particulate formulations of poorly water-soluble drugs by using a novel optimized technique. Eur J Pharm Biopharm. 2006;63:173–5.

Douroumis D, Scheler S, Fahr A. Using a modified Shepards method for optimization of a nanoparticulate cyclosporine a formulation prepared by a static mixer technique. J Pharm Sci. 2008;97:919–30.

Dua J, Lib X, Zhaoc H, Zhoua Y, Wanga L, Tiana S, Wanga Y. Nanosuspensions of poorly water-soluble drugs prepared by bottom-up technologies. Int J Pharm. 2015;495:738–49.

Ehrfeld W, Golbig K, Hessel V, Löwe H, Richter T. Characterization of mixing in micromixers by a test reaction: single mixing units and mixer arrays. Ind Eng Chem Res. 1999;38:1075–82.

El-Gendy N, Aillon K, Berkland C. Dry powdered aerosols of diatrizoic acid nanoparticle agglomerates as a lung contrast agent. Int J Pharm. 2010;391:305–12.

Erdemir D, Lee A, Myerson A. Nucleation of crystals from solution: classical and two-step models. Acc Chem Res. 2009;42:621–9.

Fu Q, Sun J, Ai X, Zhang P, Li M, Wang Y, Liu X, Sun Y, Sui X, Sun L. Nimodipine nanocrystals for oral bioavailability improvement: role of mesenteric lymph transport in the oral absorption. Int J Pharm. 2013;448:290–7.

Gandhi P, Murthy Z. Solubility and crystal size of sirolimus in different organic solvents. J Chem Eng Data. 2010;55:5050–4.

Ganta S, Paxton JW, Baguley BC, Garg S. Formulation and pharmacokinetic evaluation of an asulacrine nanocrystalline suspension for intravenous delivery. Int J Pharm. 2009;367:179–86.

Gao L, Zhang D, Chen M. Drug nanocrystals for the formulation of poorly soluble drugs and its application as a potential drug delivery system. J Nanopart Res. 2008;10:845–62.

Gao L, Liu GY, Ma JL, Wang XQ, Zhou L, Li X. Drug nanocrystals: in vivo performances. J Control Release. 2012;30:307–24.

Gao W, Chen Y, Thompson DH, Park K, Li T. Impact of surfactant treatment of paclitaxel nanocrystals on biodistribution and tumor accumulation in tumor-bearing mice. J Control Release. 2016;237:168–76.

Garmise RJ, Mar K, Crowder TM, Hwang R, Ferriter M, Huang J, Mikszta JA, Sullivan VJ, Hickey AJ. Formulation of a dry powder influenza vaccine for nasal delivery. AAPS Pharm Sci Tech. 2006;7(1):E131–7.

Gassmann P, List M, Schweitzer A, Sucker H. Hydrosols: alternatives for the parenteral application of poorly water soluble drugs. Eur J Pharm Biopharm. 1994;40:64–72.

Gigliobianco MS, Casadidio C, Censi R, Martino PD. Nanocrystals of poorly soluble drugs: drug bioavailability and physiochemical stability. Pharmaceutics. 2018;10(134):1–29.

Gindy M, Panagiotopoulos A, Prud'homme R. Composite block copolymer stabilized nanoparticles: simultaneous encapsulation of organic actives and inorganic nanostructures. Langmuir. 2008a;24:83–90.

Gindy M, Ji S, Hoye T, Panagiotopoulos A, Prud'homme R. Preparation of poly(ethylene glycol) protected nanoparticles with variable bioconjugate ligand density. Biomacromolecules. 2008b;9:2705–11.

Gindy M, Hoye S, Panagiotopoulos A, Prud'homme R. Preparation of poly(ethylene glycol) protected nanoparticles with variable bioconjugate ligand density. Biomacromolecules. 2008c;9:2705–11.

Gradl J, Schwarzer H, Schwertfirm F, Manhart M, Peukert W. Precipitation of nanoparticles in a T-mixer: coupling the particle population dynamics with hydrodynamics through direct numerical simulation. Chem Eng Process. 2006;45:908–16.

Granberg R, Ducreux C, Gracin S, Rasmuson A. Primary nucleation of paracetamol in acetone–water mixtures. Chem Eng Sci. 2001;56:2305–13.

Gu CH, Grant DJ. Estimating the relative stability of polymorphs and hydrates from heats of solution and solubility data. J Pharm Sci. 2001;90(9):1277–87.

Gulsun T, Gursoy RN, Levent O. Nanocrystal technology for oral delivery of poorly water-soluble drugs. FARAD J Pharm Sci. 2009;34:55–65.

Guo Z, Zhang M, Li H, Wang J, Kougoulos E. Effect of ultrasound on anti-solvent crystallization process. J Cryst Growth. 2005;273:555–63.

Hancock BC, Parks M. What is the true solubility advantage for amorphous pharmaceuticals? Pharm Res. 2000;17(4):397–404.

He Y, Huang Y, Cheng Y. Structure evolution of curcumin nanoprecipitation from a micromixer. Cryst Growth Des. 2010;10:1021–4.

He Y, Huang Y, Wang W, Cheng Y. Integrating micromixer precipitation and electrospray drying toward continuous production of drug nanoparticles. Chem Eng J. 2011;168:931–7.

Helmholtz RV. Untersuchungen über Dämpfe und Nebel, besonders über solche von Lösungen (Investigations of vapors and mists, and especially of such things from solutions). Ann Phys. 1886;263(4):508–43.

Hu T, Chiou H, Chan H, Chen J, Yun J. Preparation of inhalable salbutamol sulphate using reactive high gravity controlled precipitation. J Pharm Sci. 2008;97:944–9.

Hu J, Ng W, Dong Y, Shen S, Tan R. Continuous and scalable process for water-redispersible nanoformulation of poorly aqueous soluble APIs by antisolvent precipitation and spray-drying. Int J Pharm. 2011;404:198–204.

Huang X, Peng X, Wang Y, Wang Y, Shin DM, El-Sayed MA, Nie S. A reexamination of active and passive tumor targeting by using rod-shaped gold nanocrystals and covalently conjugated peptide ligands. ACS Nano. 2010;4:5887–96.

Ige PP, Baria RK, Gattani SG. Fabrication of fenofibrate nanocrystals by probe sonication method for enhancement of dissolution rate and oral bioavailability. Colloids Surf B Biointerfaces. 2013;108:366–73.

Jayasankar A, Somwangthanaroj A, Shao ZJ, Rodríguez-Hornedo N. Cocrystal formation during cogrinding and storage is mediated by amorphous phase. Pharm Res. 2006;23(10):2381–92.

Jermain SV, Brough C, Williams RO. Amorphous solid dispersions and nanocrystal technologies for poorly water-soluble drug delivery-an update. Int J Pharm. 2018;535:379–92.

Johnson B. Flash Nanoprecipitation of organic actives via confined micromixing and block copolymer stabilization. Princeton: Princeton University; 2003.

Johnson B, Prud'homme R. Chemical processing and micromixing in confined impinging jets. AICHE J. 2003a;49:2264–82.

Johnson B, Prud'homme R. Flash nanoprecipitation of organic actives and block copolymers using a confined impinging jets mixer. Aust J Chem. 2003b;56:1021–4.

Jones A. Crystallization process systems. Oxford/Boston: Butterworth-Heinemann; 2002.

Jones A, Mullin J. Programmed cooling crystallization of potassium sulphate solutions. Chem Eng Sci. 1974;29:105–18.

Junghanns J-UA, Müller RH. Nanocrystal technology, drug delivery and clinical applications. Int J Nanomed. 2008;3(3):295–310.

Junyaprasert VB, Morakul B. Nanocrystals for enhancement of oral bioavailability of poorly water-soluble drugs. Asian J Pharm Sci. 2015;10(1):13–23.

Karmwar P, Graeser K, Gordon KC, Strachan CJ, Rades T. Investigation of properties and recrystallisation behaviour of amorphous indomethacin samples prepared by different methods. Int J Pharm. 2011;417(1–2):94–100.

Karmwar P, Graeser K, Gordon KC, Strachan CJ, Rades T. Effect of different preparation methods on the dissolution behaviour of amorphous indomethacin. Eur J Pharm Biopharm. 2012;80(2):459–64.

Keck CM, Müller RH. Drug nanocrystals of poorly soluble drugs produced by high pressure homogenization. Eur J Pharm Biopharm. 2006;62:3–16.

Kelly R, Rodr'guez-Hornedo N. Solvent effects on the crystallization and preferential nucleation of carbamazepine anhydrous polymorphs: a molecular recognition perspective. Org Process Res Dev. 2009;13:1291–300.

Kesisoglou F, Panmai S, Wu Y. Nanosizing – oral formulation development and biopharmaceutical evaluation. Adv Drug Deliv Res. 2007;59:631–44.

Khan MS, Vishakante GD, Bathool A. Development and characterization of pilocarpine loaded Eudragit nanosuspensions for ocular drug delivery. J Biomed Nanotechnol. 2013;9:124–31.

Kim K, Mersmann A. Estimation of metastable zone width in different nucleation processes. Chem Eng Sci. 2001;56:2315–24.

Klingler C, Müller B, Steckel H. Insulin-micro- and nanoparticles for pulmonary delivery. Int J Pharm. 2009;377:173–9.

Kreuter J, Alyautdin RN, Kharkevich DA, et al. Passage of peptides through the blood – brain barrier with colloidal polymer particles nanoparticles. Brain Res. 1995;6741:171–4.

Kumar S, Burgess DJ. Nanosuspensions. In: Wright JC, Burgess DJ, editors. Long acting injections and implants. New York: Springer; 2012. p. 239–61.

Kumar V, Wang L, Riebe M, Tung H, Prud'homme R. Formulation and stability of itraconazole and odanacatib nanoparticles: governing physical parameters. Mol Pharm. 2009a;6:1118–24.

Kumar V, Hong S, Maciag A, Saavedra J, Adamson D, Prud'homme R, Keefer L, Chakrapani H. Stabilization of the nitric oxide (NO) prodrugs and anticancer leads, PABA/NO and double JS-K, through incorporation into PEG-protected nanoparticles. Mol Pharm. 2009b;7:291–8.

Kwade A. Wet comminution in stirred media mills – research and its practical application. Powder Technol. 1999;105:14–20.

LaMer V, Dinegar R. Theory, production and mechanism of formation of monodispersed hydrosols. J Am Chem Soc. 1950;72:4847–54.

Lee J. Drug nano- and microparticles processed into solid dosage forms: physical properties. J Pharm Sci. 2003;92(10):2057–68.

Li C, Le Y, Chen J. Formation of bicalutamide nanodispersion for dissolution rate enhancement. Int J Pharm. 2011;404:257–63.

Lince F, Marchisio D, Barresi A. Strategies to control the particle size distribution of poly-[epsilon]-caprolactone nanoparticles for pharmaceutical applications. J Colloid Interface Sci. 2008;322:505–15.

Lince F, Marchisio D, Barresi A. A comparative study for nanoparticle production with passive mixers via solvent-displacement: use of CFD models for optimization and design. Chem Eng Process. 2011;50:356–68.

Lindenberg C, Mazzotti M. Effect of temperature on the nucleation kinetics of [alpha] l-glutamic acid. J Cryst Grow. 2009;311:1178–84.

Lindfors L, Skantze P, Skantze U, Westergren J, Olsson U. Amorphous drug nanosuspensions. 3. Particle dissolution and crystal growth. Langmuir. 2007;23:9866–74.

Lindfors L, Forssén S, Westergren J, Olsson U. Nucleation and crystal growth in supersaturated solutions of a model drug. J Colloid Interface Sci. 2008;325:404–13.

Liu Y, Kathan K, Saad W, Prud'homme R. Ostwald ripening of beta-carotene nanoparticles. Phys Rev Lett. 2007;98:036102.

Liu Y, Cheng C, Prud'homme R, Fox R. Mixing in a multi-inlet vortex mixer (MIVM) for flash nanoprecipitation. Chem Eng Sci. 2008;63:2829–42.

Liu Y, Huang L, Liu F. Paclitaxel nanocrystals for overcoming multidrug resistance in cancer. Mol Pharm. 2010a;7:863–9.

Liu Z, Huang Y, Jin Y, Cheng Y. Mixing intensification by chaotic advection inside droplets for controlled nanoparticle preparation. Microfluid Nanofluid. 2010b;9:773–86.

Liu P, Rong X, Laru J, Van Veen B, Kiesvaara J, Laaksonen T, Peltonen L. Nanosuspensions of poorly soluble drugs: preparation and development by wet milling. Int J Pharm. 2011;411:215–22.

Liu Y, Xie P, Zhang D, Zhang Q. A mini review of nanosuspensions development. J Drug Target. 2012;20(3):209–23.

Liu P, De Wolf O, Laru J, Heikkilä T, Van Veen B, Kiesvaara J, Hirvonen J, Peltonen L, Laaksonen T. Dissolution studies of poorly soluble drug nanosuspensions in non-sink conditions. AAPS PharmSciTech. 2013;14:748–56.

Liu T, Han M, Tian F, Cun D, Rantanen J, Yang M. Budesonide nanocrystal-loaded hyaluronic acid microparticles for inhalation: in vitro and in vivo evaluation. Carbohydr Polym. 2018;181:1143–52.

Liversidge GG, Cundy KC. Particle size reduction for improvement of oral bioavailability of hydrophobic drugs. I. Absolute oral bioavailability of nanocrystalline danazol in beagle dogs. Int J Pharm. 1995;125:91–7.

Loftsson T, Brewster ME. Pharmaceutical applications of cyclodextrins: basic science and product development. J Pharm Pharmacol. 2010;62:1607–21.

Lu Y, Ye L, Wu W. Injected nanocrystals for targeted drug delivery. Acta Pharm Sin B. 2016a;6(2):106–13.

Lu Y, Li Y, Wu W. Injected nanocrystals for targeted drug delivery. Acta Pharm Sin B. 2016b;6:106–13.

Lyczko N, Espitalier F, Louisnard O, Schwartzentruber J. Effect of ultrasound on the induction time and the metastable zone widths of potassium sulphate. Chem Eng J. 2002;86:233–41.

Mahajan A, Kirwan D. Rapid precipitation of biochemical. J Phys D Appl Phys. 1993;26:176–80.

Mahajan A, Kirwan D. Micromixing effects in a two-impinging-jets precipitator. AICHE J. 1996;42:1801–14.

Malamatari M, Taylor MG, Malamataris S, Douroumis D, Kachrimanis K. Pharmaceutical nanocrystals: production by wet milling and applications. Drug Discov Today. 2018;00(00):1–14.

Matteucci M, Hotze M, Johnston K, Williams R. Drug nanoparticles by antisolvent precipitation: mixing energy versus surfactant stabilization. Langmuir. 2006;22:8951–9.

Matteucci M, Paguio J, Miller M, Williams R III, Johnston K. Flocculated amorphous nanoparticles for highly supersaturated solutions. Pharm Res. 2008;25:2477–87.

Mauludin R, Müller RH, Keck CM. Development of an oral rutin nanocrystal formulation. Int J Pharm. 2009;370:202–9.

Mellaerts R, Mols R, Kayaert P, Annaert P, Van Humbeeck J, Van den Mooter G, Martens JA, Augustijns P. Ordered mesoporous silica induces pH-independent supersaturation of the basic low solubility compound itraconazole resulting in enhances transepithelial transport. Int J Pharm. 2008;357:169–79.

Meng X, Chen Y, Chowdhury S, Yang D, Mitra S. Stabilizing dispersions of hydrophobic drug molecules using cellulose ethers during anti-solvent synthesis of micro-particulates. Colloids Surf B Biointerfaces. 2009;70:7–14.

Merisko-Liversidge E, Liversidge GG. Nanosizing for oral and parenteral drug delivery: a perspective on formulating poorly-water soluble compounds using wet media milling technology. Adv Drug Deliv Rev. 2011;63:427–40.

Merisko-Liversidge E, Sarpotdar P, Bruno J, Hajj S, Wei L, Peltier N, Rake J, Shaw J, Pugh S, Polin L. Formulation and antitumor activity evaluation of nanocrystalline suspensions of poorly soluble anticancer drugs. Pharm Res. 1996;13:272–8.

Mitri K, Shegokar R, Gohla S, Anselmi C, Müller RH. Lutein nanocrystals as antioxidant formulation for oral and dermal delivery. Int J Pharm. 2011;420:141–6.

Moschwitzer JP. Drug nanocrystals in the commercial pharmaceutical development process. Int J Pharm. 2013;453(1):142–56.

Moschwitzer J, Muller RH. Spray coated pellets as carrier system for mucoadhesive drug nanocrystals. Eur J Pharm Biopharm. 2006;62:282–7.

Muller RH, Keck CM. Challenges and solutions for the delivery of biotech drugs – a review of drug nanocrystal technology and lipid nanoparticles. J Biotechnol. 2004;113:151–70.

Müller RH, Keck CM. Twenty years of drug nanocrystals: where are we, and where do we go? Eur J Pharm Biopharm. 2012;80:1–3.

Muller RH, Jacobs C, Kayser O. Nanosuspensions as particulate drug formulations in therapy. Rationale for development and what we can expect for the future. Adv Drug Deliv Rev. 2001;47:3–19.

Müller RH, Jacobs C, Kayser O. Nanosuspensions as particulate drug formulations in therapy: rationale for development and what we can expect for the future. Adv Drug Deliv Rev. 2001;47:3–19.

Mullin J, Nyvlt J. Programmed cooling of batch crystallizers. Chem Eng Sci. 1971;26:369–77.

Muntó M, Sala S, Cano M, Gimeno M, Ventosa N, Veciana J. New technologies for the preparation of micro- and nanostructured materials with potential applications in drug delivery and clinical diagnostics. Contrib Sci. 2005;3:11–8.

Murnane D, Marriott C, Martin G. Developing an environmentally benign process for the production of microparticles: amphiphilic crystallization. Eur J Pharm Biopharm. 2008;69:72–82.

Niwa T, Nakanishi Y, Danjo K. One-step preparation of pharmaceutical nanocrystals using ultra cryomilling technique in liquid nitrogen. Eur J Pharm Sci. 2010;41(1):78–85.

Noyes A, Whitney W. The rate of solution of solid substances in their own solutions. J Am Chem Soc. 1897;19:930–4.

Omar W, Mohnicke M, Ulrich J. Determination of the solid liquid interfacial energy and thereby the critical nucleus size of paracetamol in different solvents. Cryst Res Technol. 2006;41:337–43.

Otte A, Carvajal MT. Assessment of milling-induced disorder of two pharmaceutical compounds. J Pharm Sci. 2011;100:1793–804.

Owais M, Zia Q, Jamal F, Zubair S. Nanocrystal based therapeutics: scope and potential application in health sciences. Nanomed Nanotechnol J. 2019;2(1):122.

Panagiotou T, Mesite S, Fisher R. Production of norfloxacin nanosuspensions using microfluidics reaction technology through solvent/antisolvent crystallization. Ind Eng Chem Res. 2009;48:1761–71.

Patravale V, Date AA, Kulkarni R. Nanosuspensions: a promising drug delivery strategy. J Pharm Pharmacol. 2004;56:827–40.

Pattekari P, Zheng Z, Zhang X, Levchenko T, Torchilin V, Lvov Y. Top-down and bottom-up approaches in production of aqueous nanocolloids of low solubility drug paclitaxel. Phys Chem Chem Phys. 2011;13:9014–9.

Pawar VK, Singh Y, Meher JG, Gupta S, Chourasia MK. Engineered nanocrystal technology: in-vivo fate, targeting and applications in drug delivery. J Control Release. 2014;183:51–66.

Peltonen L, Hirvonen J. Pharmaceutical nanocrystals by nanomilling: critical process parameters, particle fracturing and stabilization methods. J Pharm Pharmacol. 2010;62:1569–79.

Peltonen L, Hirvonen J. Drug nanocrystals – versatile option for formulation of poorly soluble materials. Int J Pharm. 2018;537(1–2):73–83.

Stenger F, Peukert W. The role of particle interactions on suspension rheology – application to submicron grinding in stirred ball mills. Chem Eng Technol. 2003;26:177–83.

Rabinow BE. Nanosuspensions in drug delivery. Nat Rev Drug Discov. 2004;3:785–96.

Rawat RS. Dense plasma focus – from alternative fusion source to versatile high energy density plasma source for plasma nanotechnology. J Phys Conf Ser. 2015;591:012021.

Rijesh M, Deepak A, Dev K, Surendranathan AO, Sreekanth MS. Effect of milling time on production of aluminium nanoparticle by high energy ball milling. Int J Mech Eng Technol. 2018;9(8):646–52.

Salem H. Sustained-release progesterone nanosuspension following intramuscular injection in ovariectomized rats. Int J Nanomedicine. 2010;5:943–54.

Salem H, Abdelrahim M, Eid K, Sharaf M. Nanosized rods agglomerates as a new approach for formulation of a dry powder inhaler. Int J Nanomed. 2011a;6:311–20.

Salem H, Abdelrahim M, Eid K, Sharaf M. Nanosized rods agglomerates as a new approach for formulation of a dry powder inhaler. Int J Nanomedicine. 2011b;6:311–20.

Schöll J, Lindenberg C, Vicum L, Mazzotti M, Brozio J. Antisolvent precipitation of PDI 747: kinetics of particle formation and growth. Cryst Growth Des. 2007;7:1653–61.

Sharma S, Singh J, Verma A, Teja V, Shukla RP, Singh S, Sharma V, Konwar R, Mishra P. Hyaluronic acid anchored paclitaxel nanocrystals improves chemotherapeutic efficacy and inhibits lung metastasis in tumor-bearing rat model. RSC Adv. 2016;6:73083–95.

Shegokar R, Singh KK. Surface modified nevirapine nanosuspensions for viral reservoir targeting: in vitro and in vivo evaluation. Int J Pharm. 2011;421:341–52.

Shekunov B, Baldyga J, York P. Particle formation by mixing with supercritical antisolvent at high Reynolds numbers. Chem Eng Sci. 2001;56:2421–33.

Sheng JJ, Sirois PJ, Dressman JB, Amidon GL. Particle diffusional layer thickness in a USP dissolution apparatus II: a combined function of particle size and paddle speed. J Pharm Sci. 2007;97:4815–29.

Shubar HM, Lachenmaier S, Heimesaat MM, Lohman U, Mauludin R, Mueller RH, Fitzner R, Borner K, Liesenfeld O. SDS-coated atovaquone nanosuspensions show improved therapeutic efficacy against experimental acquired and reactivated toxoplasmosis by improving passage of gastrointestinal and blood-brain barriers. J Drug Target. 2011;19:114–24.

Sigfridsson K, Forssén S, Holländer P, Skantze U, Verdier J. A formulation comparison, using a solution and different nanosuspensions of a poorly soluble compound. Eur J Pharm Biopharm. 2007;67:540–7.

Söhnel O, Garside J. Precipitation: basic principles and industrial applications. Boston: Butterworth-Heinemann; 1992.

Sugimoto T. Formation of monodispersed nano- and micro-particles controlled in size, shape, and internal structure. Chem Eng Tech. 2003;26:313–21.

Sugimoto S, Niwa T, Nakanishi Y, Danjoa K. Development of a novel ultra cryo-milling technique for a poorly water-soluble drug using dry ice beads and liquid nitrogen. Int J Pharm. 2012a;426:162–9.

Sugimoto S, Niwa T, Nakanishi Y, Danjoa K. Novel ultra-cryo milling and co-grinding technique in liquid nitrogen to produce dissolution-enhanced nanoparticles for poorly water-soluble drugs. Chem Pharm Bull. 2012b;60:325–33.

Sultana S, Talegaonkar S, Ali R, Mittal G, Bhatnagar A, Ahmad F. Formulation development and optimization of alpha ketoglutarate nanoparticles for cyanide poisoning. Powder Technol. 2011;211:1–9.

Sun Y. Supercritical fluid technology in materials science and engineering: syntheses, properties, and applications. New York: Marcel Dekker; 2002.

Teychene S, Biscans B. Nucleation kinetics of polymorphs: induction period and interfacial energy measurements. Cryst Growth Des. 2008;8:1133–9.

Thanki K, Gangwal RP, Sangamwar AT, Jain S. Oral delivery of anticancer drugs: challenges and opportunities. J Control Release. 2013;170:15–40.

Thybo P, Hovgaard L, Lindeløv J, Brask A, Andersen S. Scaling up the spray drying process from pilot to production scale using an atomized droplet size criterion. Pharm Res. 2008;25:1610–20.

Trapani G, Denora N, Trapani A, Laquintana V. Recent advances in ligand targeted therapy. J Drug Target. 2012;20:1–22.

Trasi NS, Byrn SR. Mechanically induced amorphization of drugs: a study of the thermal behavior of cryomilled compounds. AAPS PharmSciTech. 2012;13:772–84.

Uemoto Y, Toda S, Adachi A, Kondo K, Niwa T. Ultra cryo-milling with liquid nitrogen and dry ice beads: characterization of dry ice as milling beads for application to various drug compounds. Chem Pharm Bull. 2018;66(8):794–804.

Valencia P, Basto P, Zhang L, Rhee M, Langer R, Farokhzad O, Karnik R. Single-step assembly of homogenous lipid-polymeric and lipid-quantum dot nanoparticles enabled by microfluidic rapid mixing. ACS Nano. 2010;4:1671–9.

Van Eerdenbrugh B, Froyen L, Van Humbeeck J, Martens JA, Augustijns P, Van den Mooter G. Drying of crystalline drug nanosuspensions the importance of surface hydrophobicity on dissolution behavior upon redispersion. Eur J Pharm Sci. 2008;35(1):127–35.

Verma S, Gokhale R, Burgess D. A comparative study of top-down and bottom-up approaches for the preparation of micro/nanosuspensions. Int J Pharm. 2009;380:216–22.

Vidlářová L, Romero GB, Hanuš J, Štěpánek F, Müller RH. Nanocrystals for dermal penetration enhancement – effect of concentration and underlying mechanisms using curcumin as model. Eur J Pharm Biopharm. 2016;104:216–25.

Wang Q, Wang J, Yu W, Shao L, Chen G, Chen J. Investigation of micromixing efficiency in a novel high-throughput microporous tube-in-tube microchannel reactor. Ind Eng Chem Res. 2009;48:5004–9.

Wang J, Zhang Q, Zhou Y, Shao L, Chen J. Microfluidic synthesis of amorphous cefuroxime axetil nanoparticles with size-dependent and enhanced dissolution rate. Chem Eng J. 2010;162:844–51.

Wang T, Qi J, Ding N, Dong X, Zhao W, Lu Y, Wang C, Wu W. Tracking translocation of self-discriminating curcumin hybrid nanocrystals following intravenous delivery. In J Pharm. 2018;546:10–9.

Wojnarowska Z, Grzybowska K, Adrjanowicz K, Kaminski K, Paluch M, Hawelek L, Wrzalik R, Dulski M, Sawicki W, Mazgalski J, Tukalska A, Bieg T. Study of the amorphous glibenclamide drug: analysis of the molecular dynamics of quenched and cryomilled material. Mol Pharm. 2010;7(5):1692–707.

Wong S, Ward M, Wharton C. Micro T-mixer as a rapid mixing micromixer. Sensors Actuators B Chem. 2004;100:359–79.

Xia D, Quan P, Piao H, Piao H, Sun S, Yin Y, Cui F. Preparation of stable nitrendipine nanosuspensions using the precipitation–ultrasonication method for enhancement of dissolution and oral bioavailability. Eur J Pharm Sci. 2010;40:325–34.

Yadav K, Sawant K. Modified nanoprecipitation method for preparation of cytarabine-loaded PLGA nanoparticles. AAPS PharmSciTech. 2010;11:1456–65.

Yadav TP, Yadav RM, Singh DP. Mechanical milling: a top down approach for the synthesis of nanomaterials and nanocomposites. Nanosci Nanotechnol. 2012;2(3):22–48.

Yang H, Chu G, Zhang J, Shen Z, Chen J. Micromixing efficiency in a rotating packed bed: experiments and simulation. Ind Eng Chem Res. 2005;44:7730–7.

Yang W, Johnston KP, Williams RO III. Comparison of bioavailability of amorphous versus crystalline itraconazole nanoparticles via pulmonary administration in rats. Eur J Pharm Biopharm. 2010;75:33–41.

Yang C, Gao S, Dagnæs-Hansen F, Jakobsen M, Kjems J. Impact of peg chain length on the physical properties and bioactivity of PEGylated chitosan/siRNA nanoparticles in vitro and in vivo. ACS Appl Mater Interfaces. 2017;9:12203–16.

Yen F, Wu T, Tzeng C, Lin L, Lin C. Curcumin nanoparticles improve the physicochemical properties of curcumin and effectively enhance its antioxidant and antihepatoma activities. J Agric Food Chem. 2010;58:7376–82.

Zhai X, Lademann J, Keck CM, Müller RH. Dermal nanocrystals from medium soluble actives–physical stability and stability affecting parameters. Eur J Pharm Biopharm. 2014;88:85–91.

Zhang H, Wang J, Zhang Z, Le Y, Shen Z, Chen J. Micronization of atorvastatin calcium by antisolvent precipitation process. Int J Pharm. 2009a;374:106–13.

Zhang Z, Shen Z, Wang J, Zhao H, Chen J, Yun J. Nanonization of megestrol acetate by liquid precipitation. Ind Eng Chem Res. 2009b;48:8493–9.

Zhang H, Wang J, Shao L, Chen J. Microfluidic fabrication of monodispersed pharmaceutical colloidal spheres of atorvastatin calcium with tunable sizes. Ind Eng Chem Res. 2010;49:4156–61.

Zhao H, Wang J, Wang Q, Chen J, Yun J. Controlled liquid antisolvent precipitation of hydrophobic pharmaceutical nanoparticles in a microchannel reactor. Ind Eng Chem Res. 2007;46:8229–35.

Zhao H, Wang J, Zhang H, Shen Z, Yun J, Chen J. Facile preparation of danazol nanoparticles by high-gravity anti-solvent precipitation (HGAP) method. Chin J Chem Eng. 2009;17:318–23.

Zhao R, Hollis CP, Zhang H, Sun L, Gemeinhart RA, Li T. Hybrid nanocrystals: achieving concurrent therapeutic and bioimaging functionalities toward solid tumors. Mol Pharm. 2011;8:1985–91.

Zheng Z, Zhang X, Carbo D, Clark C, Nathan C, Lvov Y. Sonication-assisted synthesis of polyelectrolyte-coated curcumin nanoparticles. Langmuir. 2010;26:7679–81.

Zhi M, Wang Y, Wang J. Determining the primary nucleation and growth mechanism of cloxacillin sodium in methanol-butyl acetate system. J Cryst Grow. 2011;314:213–9.

Zhong J, Shen Z, Yang Y, Chen J. Preparation and characterization of uniform nanosized cephradine by combination of reactive precipitation and liquid anti-solvent precipitation under high gravity environment. Int J Pharm. 2005;301:286–93.

Zhu Z, Anacker J, Ji S, Hoye T, Macosko C, Prud'homme R. Formation of block copolymer-protected nanoparticles via reactive impingement mixing. Langmuir. 2007;23:10499–504.

Zhu Z, Margulis-Goshen K, Magdassi S, Talmon Y, Macosko C. Polyelectrolyte stabilized drug nanoparticles via flash nanoprecipitation: a model study with L-carotene. J Pharm Sci. 2010a;99:4295–306.

Zhu W, Wang J, Shao L, Zhang H, Zhang Q, Chen J. Liquid antisolvent preparation of amorphous cefuroxime axetil nanoparticles in a tube-in-tube microchannel reactor. Int J Pharm. 2010b;395:260–5.